

OPEN ACCESS

EDITED BY

Sadiq Umar,
University of Illinois Chicago, United States

REVIEWED BY

René Huber,
Hannover Medical School, Germany
Weihang Li,
Fourth Military Medical University, China

*CORRESPONDENCE

Xigao Cheng
✉ xigaocheng@hotmail.com

RECEIVED 15 July 2024

ACCEPTED 25 September 2024

PUBLISHED 17 October 2024

CITATION

Xu P, Li K, Yuan J, Zhao J, Pan H, Pan C, Xiong W, Tan J, Li T, Huang G, Chen X, Miao X, He D and Cheng X (2024) "Dictionary of immune responses" reveals the critical role of monocytes and the core target IRF7 in intervertebral disc degeneration. *Front. Immunol.* 15:1465126. doi: 10.3389/fimmu.2024.1465126

COPYRIGHT

© 2024 Xu, Li, Yuan, Zhao, Pan, Pan, Xiong, Tan, Li, Huang, Chen, Miao, He and Cheng. This is an open-access article distributed under the terms of the [Creative Commons Attribution License \(CC BY\)](https://creativecommons.org/licenses/by/4.0/). The use, distribution or reproduction in other forums is permitted, provided the original author(s) and the copyright owner(s) are credited and that the original publication in this journal is cited, in accordance with accepted academic practice. No use, distribution or reproduction is permitted which does not comply with these terms.

"Dictionary of immune responses" reveals the critical role of monocytes and the core target IRF7 in intervertebral disc degeneration

Peichuan Xu^{1,2}, Kaihui Li³, Jinghong Yuan^{1,2}, Jiangminghao Zhao^{1,2}, Huajun Pan^{1,2}, Chongzhi Pan^{1,2}, Wei Xiong^{1,2}, Jianye Tan^{1,2}, Tao Li^{1,2}, Guanfeng Huang^{1,2}, Xiaolong Chen^{1,2}, Xinxin Miao¹, Dingwen He¹ and Xigao Cheng^{1,2*}

¹Department of Orthopaedics, The Second Affiliated Hospital, Jiangxi Medical College, Nanchang University, Nanchang, China, ²Jiangxi Provincial Key Laboratory of Spine and Spinal Cord Disease, Nanchang University, Nanchang, China, ³Department of Stomatology, The Second Affiliated Hospital, Jiangxi Medical College, Nanchang University, Nanchang, China

Background: Intervertebral disc degeneration (IDD) is widely regarded as the primary contributor to low back pain (LBP). As an immune-privileged organ, upon the onset of IDD, various components of the nucleus pulposus (NP) are exposed to the host's immune system, accumulating cytokines. Cytokines facilitate intercellular communication within the immune system, induce immune cells polarisation, and exacerbate oxidative stress in IDD.

Methods: Machine learning was used to identify crucial immune cells. Subsequently, Immune Response Enrichment Analysis (IREA) was conducted on the key immune cells to determine their cytokine responses and polarisation states in IDD. "CellChat" package facilitated the analysis of cell-cell communication. Differential gene expression analysis, PPI network, GO and KEGG pathway enrichment analysis, GSVA, co-expressed gene analysis and key gene-related networks were also performed to explore hub genes and their associated functions. Lastly, the differential expression and functions of key genes were validated through *in vitro* and *in vivo* experiments.

Results: Through multiple machine learning methods, monocytes were identified as the crucial immune cells in IDD, exhibiting significant differentiation capacity. IREA revealed that monocytes in IDD polarize into an IFN- α 1 and IFN- β enriched Mono- α state, potentially intensifying inflammation. Cell-cell communication analysis uncovered alteration in ANNEXIN pathway and a reduction in CXCL signaling between macrophages and monocytes, suggesting immune response dysregulation. Furthermore, ten algorithms identified three hub genes. Both experiments conducted *in vitro* and *in vivo* have conclusively shown that IRF7 serves as a crucial target for the treatment of IDD, and its knockdown alleviates IDD. Eight small-molecule drugs were predicted to have therapeutic potential for IDD.

Conclusion: These findings offer a multidimensional understanding of the pathogenesis of IDD, pinpointing monocytes and key genes as potential diagnostic and therapeutic targets. They provide novel insights into potential diagnostic and therapeutic targets for IDD.

KEYWORDS

intervertebral disc degeneration, cytokine, monocytes, machine learning, single-cell sequencing, IRF7

1 Introduction

Intervertebral disc degeneration (IDD), a prevalent degenerative condition, predominantly impacts middle-aged and elderly individuals, often resulting in chronic low back pain (LBP) (1). LBP affects an estimated 80% of the world's population, significantly diminishing their quality of life and imposing a substantial economic toll on society (2). The intervertebral disc, situated between two adjacent vertebrae, comprises the annulus fibrosus (AF), nucleus pulposus (NP), and cartilaginous endplate (CEP) located above and below the vertebrae (3, 4). The NP, a gelatinous core, primarily comprises water, proteoglycans, and collagen. It withstands and distributes pressure while maintaining the height and hydration of the intervertebral disc through its high osmotic pressure properties (5).

During disc degeneration, the NP's ability to synthesize proteoglycans and collagen decreases, leading to reduced moisture content and impaired pressure resistance. At the same time, there is an increased expression of inflammatory mediators and proteases within the NP, which degrade the extracellular matrix (ECM), further compromising the structural integrity of the disc (6, 7). These biochemical changes can also trigger or exacerbate the inflammatory response, creating a vicious cycle that accelerates disc degeneration (8). Thus, it is essential to explore the pathological mechanisms of IDD and identify targets for nucleus pulposus cells (NPCs) dysfunction to develop effective diagnostic and therapeutic strategies for IDD.

Since its formation, the NP has been encapsulated by the AF and the CEP, creating a unique structure that isolates the NP from the host's immune system. Thus, the intervertebral disc is recognized as an immune-privileged organ (9). During IDD, various components of the NP can elicit an autoimmune response upon exposure to the host's immune system, resulting in vascular infiltration and the aggregation of inflammatory cytokines that disrupt the homeostasis of the disc (10, 11).

Cytokines, a wide range of small secreted proteins, bind to homologous receptors on target cells, mediate intercellular communication within the immune system, and are essential therapeutic targets (12, 13). Natural disc cells produce numerous cytokines up-regulated during IDD, driving many metabolic processes of disc degeneration (14–16). Phillips et al. have shown

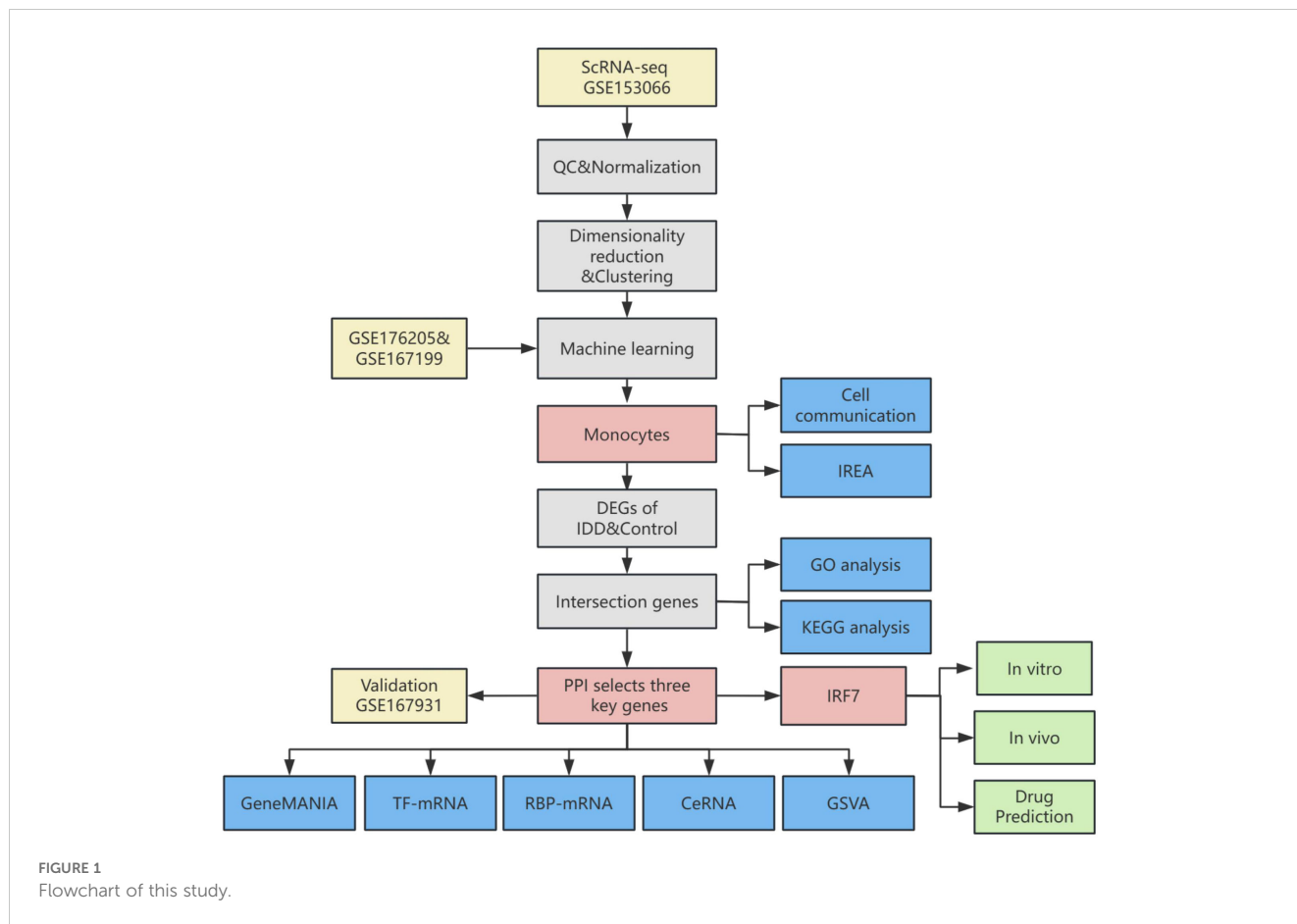
that NPCs produce multiple cytokines and chemokine receptors and can exhibit paracrine and autocrine response modes (17). These cytokines further promote IDD progression by activating intracellular signaling pathways (18, 19). During IDD progression, these cytokines may up-regulate neurotrophic and angiogenic factors, leading to angiogenesis and innervation (20, 21). Thus, the role of cytokines in the progression of IDD cannot be ignored. Cytokine-based therapies and antagonists treat various diseases, including cancer and autoimmune diseases (22). Numerous studies have highlighted the central role of cytokines in immunity. However, previous studies have often lacked a comprehensive view of each immune cell type for each cytokine. Ang Cui et al. mapped the global view of “immune-cytokine” correspondences on a single-cell scale, creating a “Dictionary of immune responses” (22). This “dictionary” can identify the most active cytokines in disease and how different immune cells perform different functions depending on the cytokine signals they receive. Its emergence provides a new perspective for studying cytokine-immune cell polarisation in diseases and helps better understand the roles of immune cells in disease development.

In this study, a multifaceted bioinformatics approach was employed to explore the role of cytokine-driven monocytes polarisation in the immune system and identify essential genes that could impact the disease, suggesting potential therapeutic targets for alleviating IDD.

2 Methods

2.1 Transcriptome data sources

The flowchart depicted in Figure 1 outlines the systematic approach undertaken in this study. All datasets employed for this research are accessible to the public, ensuring transparency and reproducibility. The transcriptome data were sourced from the publicly accessible Gene Expression Omnibus (GEO) database at <https://www.ncbi.nlm.nih.gov/geo/>. High-throughput sequencing data from GSE176205 and GSE167199 were corrected for batch effects using the “sva” package (version 3.42.0) in R (23). The sequencing platform for GSE176205 was GPL20301 Illumina HiSeq 4000 (Homo sapiens), which included 6 IDD and 3 standard control NP samples. The sequencing platform for GSE167199 was GPL24676 Illumina



NovaSeq 6000 (Homo sapiens), including 3 IDD and 3 standard control NP samples. GSE167931 was utilized as an additional dataset for validation purposes, sequenced on the GPL20795 HiSeq X Ten (Homo sapiens) platform, and included 5 IDD and 4 standard control NP samples.

2.2 Download and processing of single-cell sequencing data

A single-cell sequencing dataset was retrieved from the GEO database, which contained 16 samples (8 IDD and 8 standard control NP samples). The “Seurat” R package (version 4.2.0) was employed in the R to import the raw data within GSE153066 from the database (24). Filtering out low-quality cells and genes involved applying stringent criteria to ensure data quality: 1) Cells that failed to express at least 200 genes were excluded. 2) Cells with a mitochondrial gene expression percentage below 25% were also retained. 3) Cells with fewer than 4,000 expressed genes were retained. 4) Cells with a UMI reading of fewer than 10,000 were retained. The data were normalized using the “Seurat” R package. Following normalization, balancing average expression and dispersion was employed to pinpoint highly variable genes. Principal component analysis (PCA) yielded significant

PCs, which served as input for graph-based clustering. A harmony approach was used to eliminate batch effects across samples. For clustering, the “FindClusters” function, leveraging the optimized Shared Nearest Neighbor (SNN) modular clustering algorithm, was applied to identify 16 distinct clusters with a resolution of 0.5. The “RunUMAP” function was used for Uniform Manifold Approximation and Projection (UMAP). UMAP-1 and UMAP-2 visualized cell aggregation, subsequently enabling the identification of cell clusters based on their type-specific biomarkers. The “RunTSNE” function was then used for t-distributed stochastic neighbour embedding (t-SNE). t-SNE-1 and t-SNE-2 visualized T cell aggregation.

2.3 Single sample gene set enrichment analysis (ssGSEA)

ssGSEA represents an extension of Gene Set Enrichment Analysis (GSEA) and it was employed to calculate enrichment scores for each cell type in conventional transcriptome data based on a list of marker genes (25). Based on a list of marker genes for each cell type, we used “GSVA” R package (version 1.42.0) to perform ssGSEA analysis to calculate the enrichment fraction of each cell type in transcriptome data.

2.4 Machine learning

Support Vector Machine-Recursive Feature Elimination (SVM-RFE), a machine learning approach, trains subsets of features across categories to refine the set and pinpoint the most predictive genes. Utilizing the “glmnet” package in R (version 4.1.4), LASSO regression was implemented to compute and select linear models, effectively retaining only informative variables. Random forest analysis was conducted using the “RandomForest” function, where the minimum error was chosen as the mtry node value, and the stabilized image value was selected as the ntree. The results of SVM-RFE, LASSO regression, and Random forest were combined to select the key immune cells in this study.

2.5 Immune response enrichment analysis

Immune Response Enrichment Analysis (IREA) is a method Ang Cui et al. proposed to infer cytokine activity and immune cell polarisation during immunization (26). In a cell type-centric view, IREA uncovers over 66 distinct cytokine-mediated polarisation states within immune cell types, encompassing novel and previously undescribed states. IREA was used to calculate the cytokines that primarily generate a response based on the differentially expressed genes (DEGs) of vital immune cells and the polarisation states of critical immune cells in IDD.

2.6 Cell-cell communication analysis and ligand-receptor expression

Using the “CellChat” (version 1.1.3) R package, CellChat objects were constructed (27). Cell-cell communication was analyzed using the “CellChatDB.human” ligand-receptor interaction database as the reference. The “mergeCellChat” function was employed to combine the CellChat objects of each group, enabling a comparison of the interaction number and the interaction strength. The “netVisual_diffInteraction” function was used to visualize differences in the number or strength of interactions between groups and different cell types. Finally, the “netVisual_aggregate” function was used for visualization.

2.7 Identification of differentially expressed genes

The DEGs were identified utilizing the “limma” R package (version 3.50.0) (28). The screening criteria were $|\log_2\text{Fold Change}| > 1$ and adjusted p-value < 0.05 . Heatmaps were created employing the “pheatmap” R package (version 1.0.12) and clustered using euclidean distance and hierarchical clustering methods. Further, we explored the differences between the two groups in single-cell data. The “FindAllMarkers” function in the “Seurat” R package was employed to identify DEGs of vital immune cells between two groups.

2.8 Protein-protein interaction network construction

A PPI network was constructed by utilizing the Search Tool for the Retrieval of Interacting Genes (STRING) online resource (29). Sub-networks were constructed for proteins with interaction scores greater than 700, from which proteins with direct interactions with intersecting DEGs were extracted and analyzed. Afterward, PPI network analysis was executed using the Cytoscape plug-in (30). Ten algorithms (Betweenness, BottleNeck, Closeness, Degree, Eccentricity, EPC, MCC, MNC, Radiality and Stress) were used to screen the top 100 proteins in terms of importance. The intersecting proteins from these algorithms and the genes identified in the intersecting DEGs were designated as key genes.

2.9 Gene ontology (GO) and kyoto encyclopedia of genes and genomes (KEGG) pathway enrichment analysis

GO enrichment analysis includes three domains: biological process (BP), molecular function (MF), and cellular component (CC) analysis (31). The KEGG is a bioinformatics resource for identifying enriched and significantly altered metabolic pathways within gene lists (32). The genes of interest in IDD were analyzed for GO and KEGG enrichment using the R package “clusterProfiler” (version 4.2.2) (33).

2.10 GeneMANIA

The GeneMANIA website (<http://genemania.org>) forecasts associations between functionally analogous genes and pivotal genes (34). Gene interaction networks for key genes were constructed using the GeneMANIA website.

2.11 Gene set variation analysis (GSVA)

To explore the disparities in biological functionalities between the two groups, the gene set “h.all.v2023.1.Hs.symbols.gmt” sourced from the MSigDB was employed as the reference gene set. GSVA was performed using the R package “GSVA” (version 1.42.0).

2.12 Construction of ceRNA network, RBP-mRNA network, mRNA-TF network

Since the mechanism of action of competing endogenous RNA (ceRNA) in IDD remains unclear, we used miRTarBase (https://mirtarbase.cuhk.edu.cn/~miRTarBase/miRTarBase_2022/php/index.php), starbase3.0 (<https://rnasyu.com/encori>) and miRDB databases (<https://mirdb.org/index.html>) to back-predict microRNAs of key genes and to predict lncRNAs of common microRNAs of key genes, constructing a ceRNA network (35, 36).

The open-source platform (<https://starbase.sysu.edu.cn/tutorialAPI.php#RBPTarget>) was used to investigate mRNA and RNA-binding protein (RBP) expression associations.

The mRNA-TF interaction relationships between key genes were constructed using the TRRUST (Transcriptional Regulatory Relationships Unraveled by Sentence-based Text Mining) database. Networks were constructed using Cytoscape (version 3.9.1).

2.13 Cell culture and processing

We acquired human NPCs from Procell Life Science & Technology Co., Ltd (CP-H097, Wuhan, China). We cultured in F12/DMEM medium (Gibco, USA) supplemented with 1% Penicillin-Streptomycin Solution (NCM Biotech, China) and 10% fetal bovine serum (FBS; Gibco, USA). As described in previous literature, NPCs were induced using 100 μ M TBHP (Sigma-Aldrich, St. Louis, MO, USA) for 4 hours to construct the IDD model *in vitro* (37). Cells were transfected with small interfering RNA (si-RNA) to knock down IRF7 (ENSG00000185507, Gene ID: 3665) using the riboFECT CP Transfection Kit (RiboBio, Cat. No C10511-05, China).

2.14 RNA extraction and PCR

Total RNA was extracted from the cells using TRIzol (Thermo Fisher, USA) and chloroform (Thermo Fisher, USA). The purity and concentration of RNA samples were quantitatively assessed utilizing a Nanodrop One spectrophotometer (Thermo Fisher, USA). cDNA synthesis from the extracted RNA was performed using the PrimeScript RT reagent. Reverse transcription reagents were purchased from TaKaRa, and an RT-qPCR assay was conducted using an ABI 7500 Real-Time PCR machine (Thermo Fisher, USA). **Supplementary Table 1** provides the primer sequences employed in the study.

2.15 Animal model

The Ethics Committee of Nanchang University approved all experimental procedures involving animals, and all procedures followed the ARRIVE guidelines. Male Sprague-Dawley (SD) rats, aged 12 weeks, were sourced from SpePharm Biotechnology Ltd. (Beijing, China). A rat tail puncture model was established according to the protocol described in the literature (38). Rats were administered 4% sodium pentobarbital (1mL/1kg) to induce anaesthesia. Following skin sterilization, a 21-gauge needle was employed to make a vertical puncture into the Co4/5 disc of the tail, reaching a depth of approximately 5 millimeters. Upon completing the puncture, the needle was rotated in a full 360-degree motion and maintained in position for one minute. On postoperative days 1, 7, and 14, si-RNA and control agent si-NC 5 nmol (10 μ L) were delivered directly into the disc along the original puncture channel.

The health status of the rats was monitored daily after surgery. The flowchart of the animal experiment was performed by Figdraw (www.figdraw.com).

2.16 X-ray and magnetic resonance imaging (MRI)

X-rays and MRIs of the caudal intervertebral discs of rats were performed at 4 weeks postoperatively. The disc height index (DHI) score was utilized to quantify the structural integrity of the discs. This score was derived from the ratio of the intervertebral space height to the height of the neighbouring vertebral bodies observed in X-ray images. Additionally, the severity of IDD was assessed using MRI images and analyzed with the Pfirrmann grading system as a standardized reference.

2.17 HE and SO&FG staining

4 weeks post-surgery, the rats were euthanized, and their disc samples were fixed and immersed in 4% paraformaldehyde. Following the EDTA decalcification solution, the disc samples were dehydrated, embedded in paraffin, and sectioned serially. NP morphology was examined using hematoxylin-eosin (HE) and Safranin O-Fast Green (SO&FG) staining.

2.18 Immunohistochemical staining

Sections were treated with a 3% hydrogen peroxide solution to block endogenous peroxidase activity, followed by 3% bovine serum albumin (BSA; Servicebio, Cat no: GC305010). Primary antibodies used were COL2A1 (Proteintech, Cat No.28459-1-AP), MMP13 (Proteintech, Cat No.18165-1-AP), NLRP3 (Proteintech, Cat No. 19771-1-AP) and IL-1 β (Proteintech, Cat No. 16806-1-AP). These were incubated overnight at a temperature of 4°C. HRP-coupled secondary antibodies (Servicebio, Cat no: GB23303) were then used for the corresponding primary antibodies. Finally, the samples were stained using diaminobenzidine and hematoxylin to label the nucleus.

2.19 Immunofluorescence

The NPCs were fixed with 4% Paraformaldehyde Fix Solution (Biosharp, China, Cat no: BL539A) for 15 minutes. The cells were blocked with 3% BSA at room temperature for 30 minutes. Then, the cells were incubated overnight with antibodies against COL2A1, MMP13, NLRP3 and IL-1 β . After washing the samples, the secondary antibody was added and incubated at room temperature for 50 minutes (Servicebio, Cat no: GB21303). The samples were rewashed, and DAPI staining solution was added for incubation at room temperature in the dark for 10 minutes.

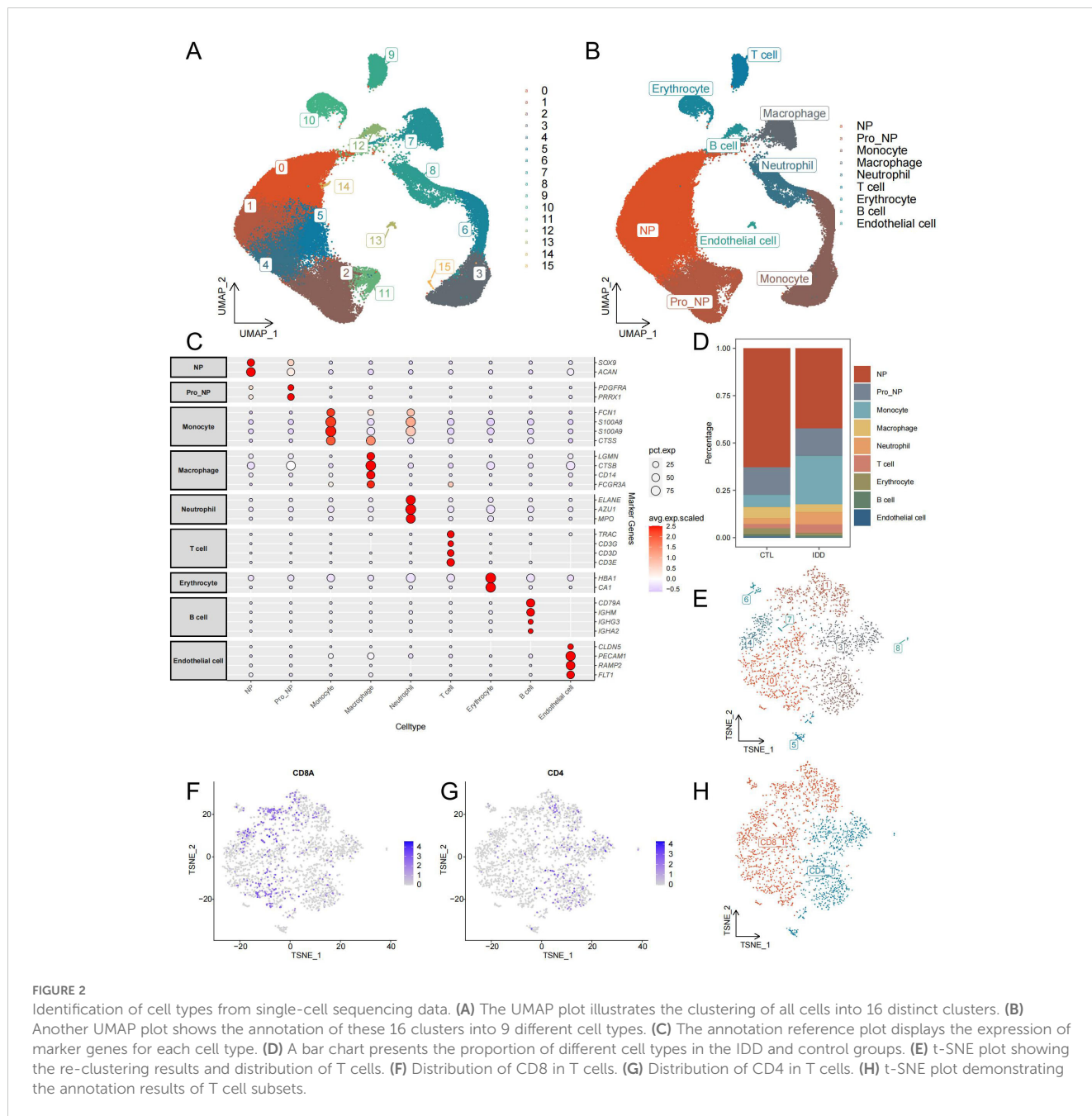


FIGURE 2 Identification of cell types from single-cell sequencing data. **(A)** The UMAP plot illustrates the clustering of all cells into 16 distinct clusters. **(B)** Another UMAP plot shows the annotation of these 16 clusters into 9 different cell types. **(C)** The annotation reference plot displays the expression of marker genes for each cell type. **(D)** A bar chart presents the proportion of different cell types in the IDD and control groups. **(E)** t-SNE plot showing the re-clustering results and distribution of T cells. **(F)** Distribution of CD8 in T cells. **(G)** Distribution of CD4 in T cells. **(H)** t-SNE plot demonstrating the annotation results of T cell subsets.

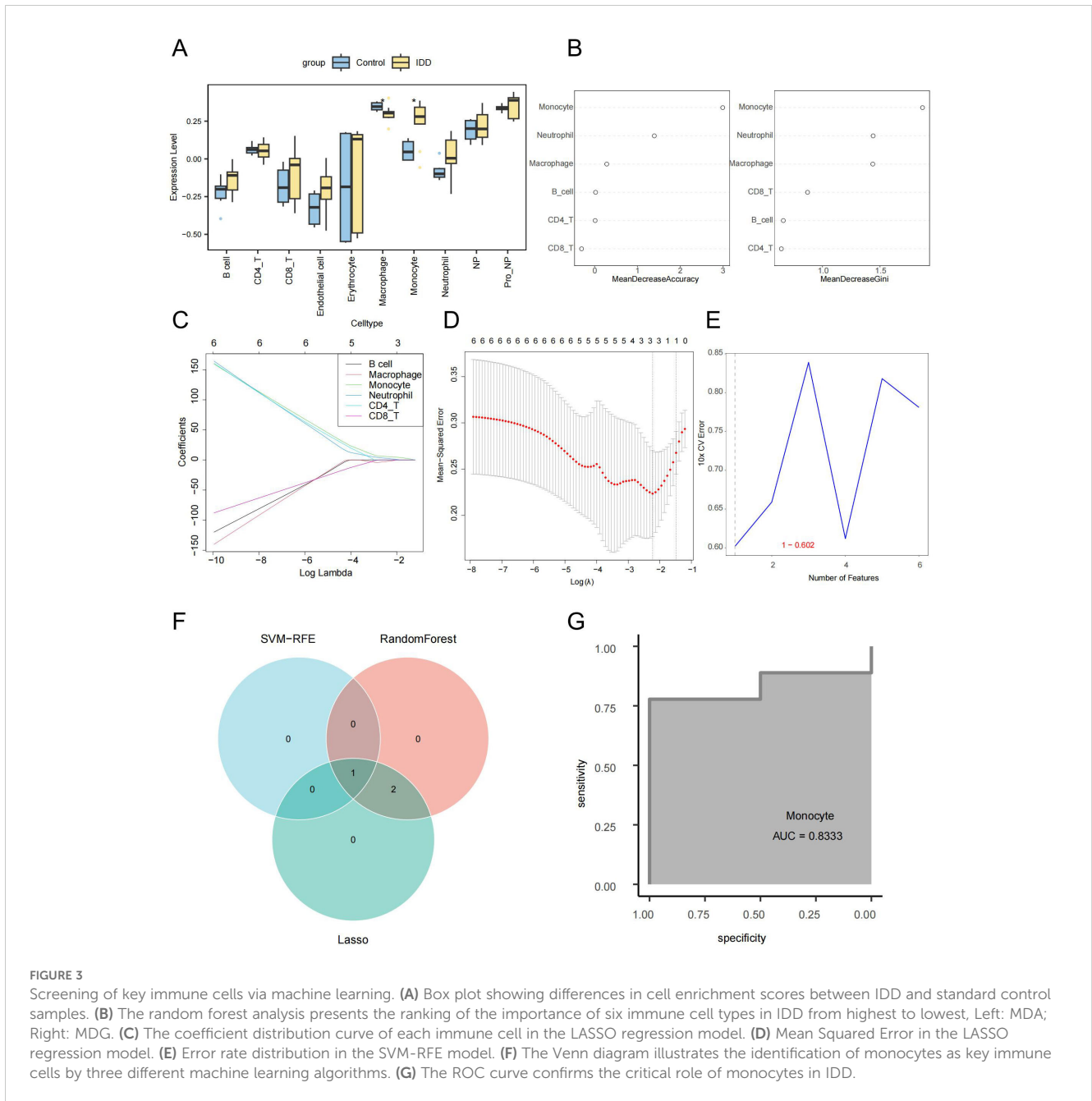
2.20 Small molecule drug prediction and molecular docking

Based on the top 20 up-regulated and 20 down-regulated genes with significant differences between the IDD group and the control group, small molecule compounds that might be effective in treating IDD were predicted using the Connectivity Map (CMAP) database. Eight compounds with the highest scores as potential drugs were selected, with toxic compounds excluded. We downloaded SDF format files for potential drugs from PubChem, PDB files of target proteins in the PDB database, and dehydrated and deligated the proteins in PyMOL. Proteins were hydrogenated in AutoDockTools (version 1.5.7). Molecular docking was then performed in

AutoDockTools. The strength of the binding energy serves as an indicator of the probability of the receptor and ligand binding together, with a decrease in binding energy corresponding to an increase in the affinity. The lower the binding energy, the more stable the conformation of the receptor became. The results of molecular docking were visualized in PyMOL.

2.21 Statistical analysis

Statistical analyses were performed utilizing R software (version 4.1.2). Spearman's correlation test were employed to examine associations between two variables. The Wilcoxon rank-sum test



was applied for comparisons between two groups, while the Kruskal-Wallis test was utilized for comparisons involving three or more groups. A statistical significance threshold was set at a p-value of less than 0.05.

3 Results

3.1 Single-cell dimensionality reduction clustering and annotation

After initial quality control and doublet removal of IDD and control samples, 65,165 cells were obtained from the single-cell dataset. All cells were aggregated into 16 clusters (Figure 2A). And

annotated by cell-specific biomarkers, we finally found 9 cell types, namely: nucleus pulposus (NP, cluster 0,1,4,5,14), progenitor nucleus pulposus (Pro_NP, cluster 2, 11), Monocyte (cluster 3,6,15), Macrophage (cluster 7), Neutrophil (cluster 8), T cell (cluster 9), Erythrocyte (cluster 10), B cell (cluster 12), and Endothelial cell (cluster 13) (Figures 2B, C). The distribution and number of different cell types varied significantly between the two groups (Figure 2D). NPCs were most reduced considerably in the IDD group, while Pro_NP, Macrophage, Erythrocyte, B cell, and Endothelial cell were also reduced to varying degrees. Monocytes increased most significantly in the IDD group, and Neutrophil also increased in IDD. T cells were re-clustered and categorized into CD4⁺ T cells and CD8⁺ T cells based on their distinct expression patterns (Figures 2E–H).

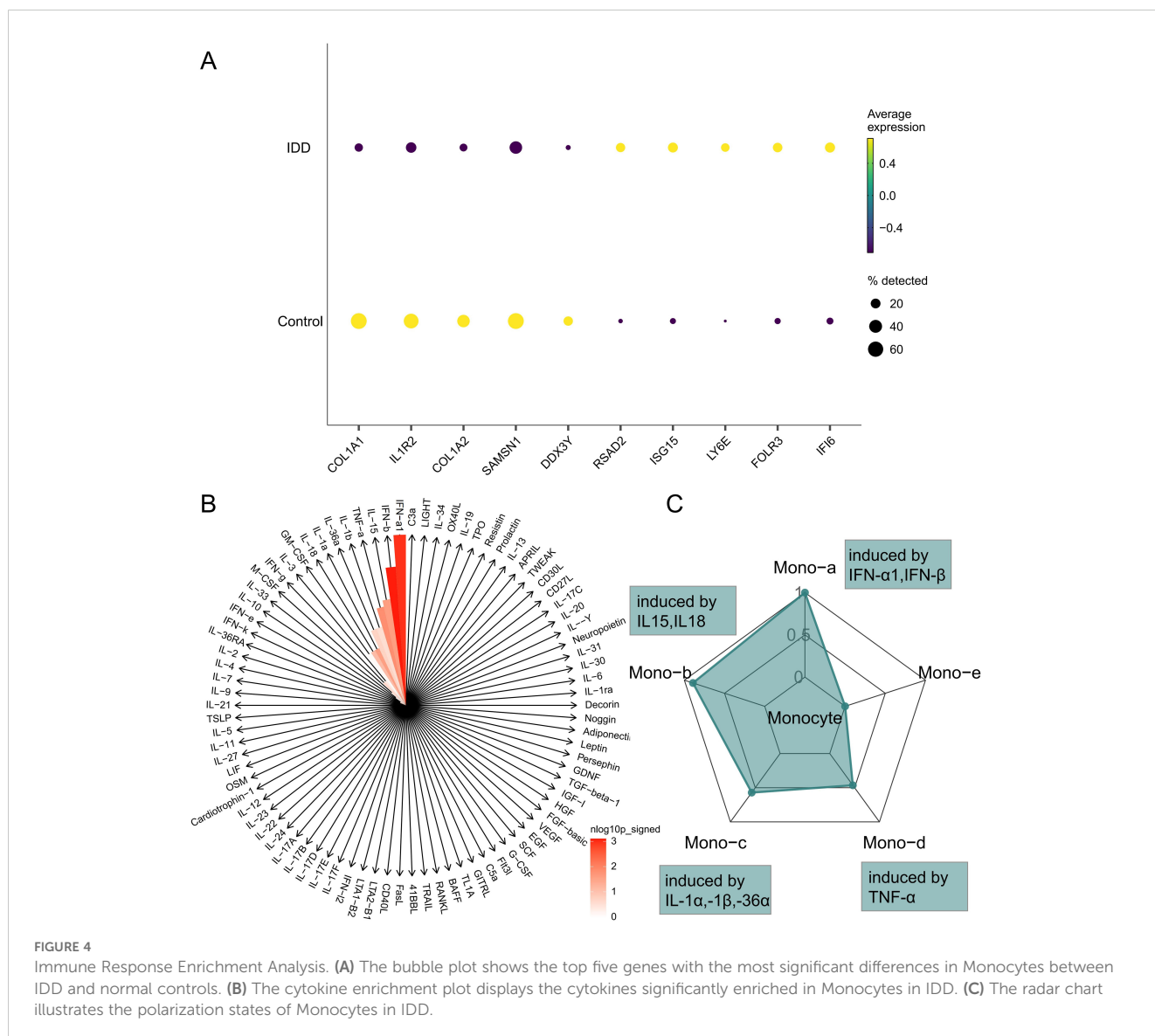
3.2 Screening of vital immune cells

The ssGSEA algorithm was used to calculate the enrichment scores of each cell type (Supplementary Table 2). There was a notable decrease in the number of macrophages in the IDD group compared to the control group. In contrast, the IDD group's monocytes count was significantly elevated compared to the control group. This is consistent with trends observed in the single-cell data (Figure 3A). The Random Forest, LASSO regression, and SVM-RFE were used to screen for critical immune cells. We selected the top 3 immune cells using the random forest algorithm based on Mean decrease accuracy (MDA) and Mean decrease Gini (MDG), which were macrophages, monocytes, and neutrophils (Figure 3B). By LASSO regression analysis, we obtained the same three types of immune cells (Figures 3C, D). However, through the SVM-RFE method, we only screened for monocytes (Figure 3E). Finally, the immune cells detected by each method were intersected, concluding that the most critical immune cell in IDD was the monocytes (Figure 3F).

The ROC curve showed that the monocytes enrichment score had good efficacy for distinguishing IDD samples from normal control samples (AUC=0.8333, Figure 3G).

3.3 Immune response enrichment analysis of key immune cells

In order to clarify the changes of cytokines in monocytes during IDD and to explore the polarization state of monocytes after receiving different cytokines, we performed a comparative analysis of monocytes between different groups to explore the immune status of monocytes in IDD (Figure 4A; Supplementary Table 3). Subsequently, IREA was conducted based on significantly up-regulated differentially expressed genes in IDD. The cytokine enrichment plot showed that monocytes in IDD were predominantly enriched for cytokines such as IFN- α 1 and IFN- β (Figure 4B; Supplementary Table 4). The cellular polarisation radar plot indicated that monocytes were primarily



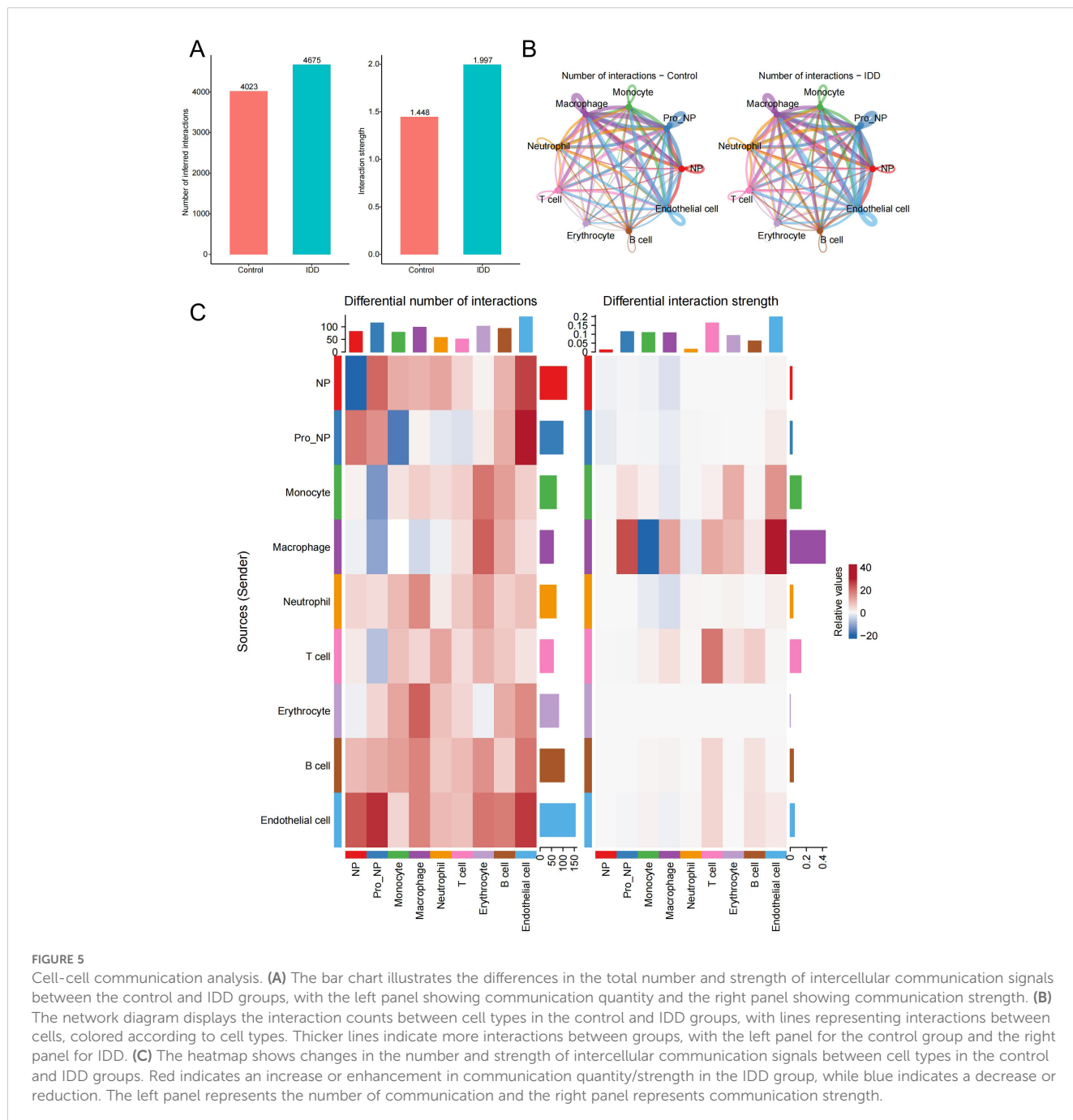
in the Mono-a polarisation state (type I interferon-induced polarisation), which may exacerbate the IDD's inflammatory response (Figure 4C; Supplementary Table 5). When IDD occurs, IFN- α 1 and IFN- β are significantly enriched in the intervertebral disc. And the monocytes are in a Mono-a polarized state, which may lead to the aggregation of inflammatory factors and matrix degradation in the intervertebral disc.

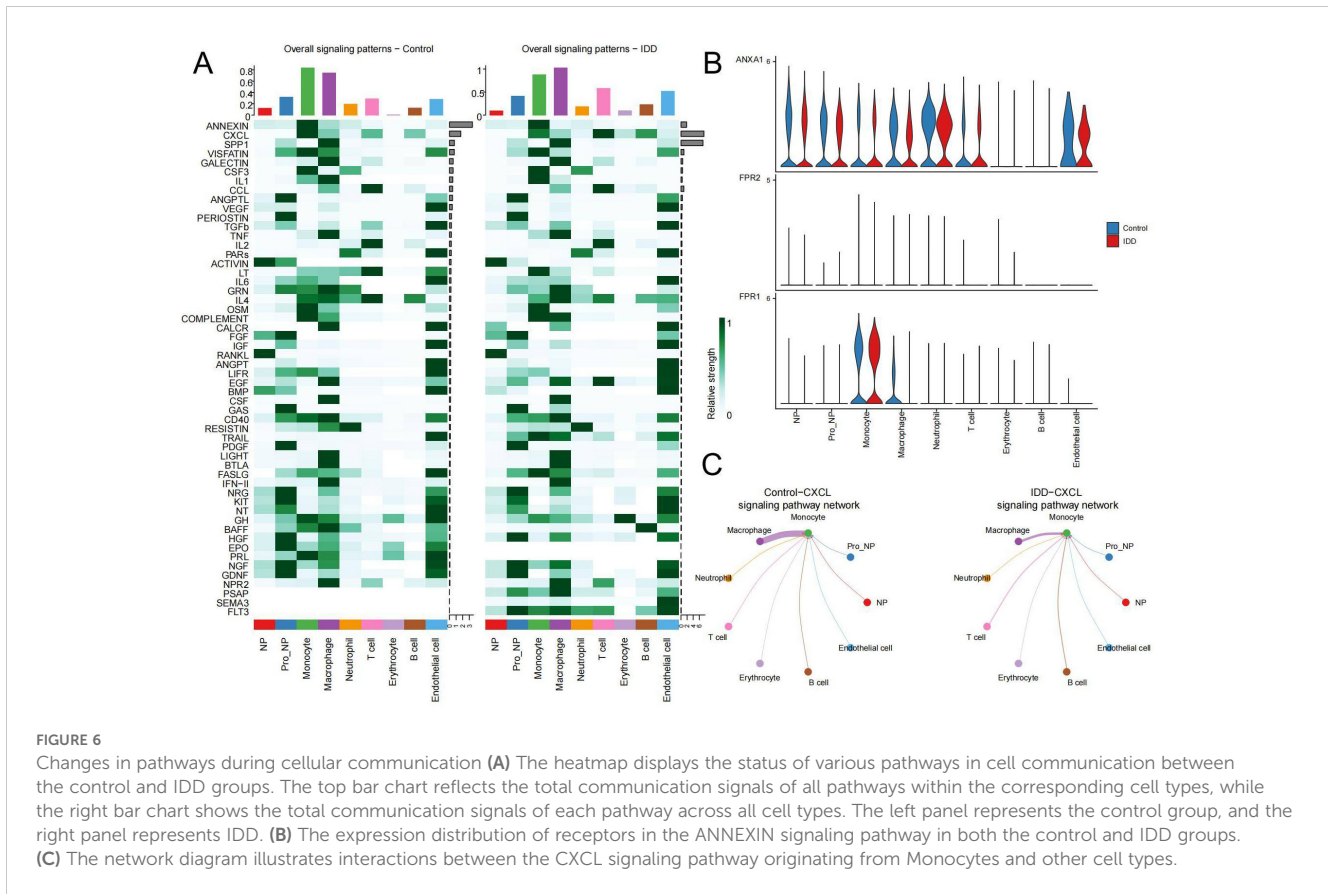
3.4 Cell-cell communication analysis

To investigate the cellular interaction network in IDD, the R package “Cellchat” was performed. Compared to the control group,

the number and the strength of interactions between different cell types were elevated in the IDD group (Figure 5A). Besides, we showed the relationship of the number of interactions between different cell types in the IDD and the control group. Relatively little difference was found between the groups (Figure 5B). Then, we focused on monocytes and found that the biggest change occurred between monocytes and macrophages. And the communication strength between the two cells decreased greatly in IDD, indicating that the interaction between macrophages and monocytes is an important factor in the occurrence of IDD (Figure 5C).

Next, we visualized the relationship between immune cells and signaling pathways in the control and IDD group in the heatmap. It demonstrated that in the control group, ANNEXIN is the most





important signaling pathway, but its communication signal decreases significantly after the occurrence of IDD (Figure 6A). To explore the reasons for this trend, violin plots were used to show the expression of the ANNEXIN pathway between the control and IDD groups. Compared with the control group, the ligand ANXA1 showed a decreasing trend in all cell types. And monocytes, with the highest expression of receptor FPR1, may be affected (Figure 6B). In addition, we also observed a significant decline in the CXCL signaling pathway in monocytes after the occurrence of IDD (Figure 6A). Thus, the CXCL pathway-mediated communication between monocytes and other cells was mapped. The results showed that the CXCL pathway of monocytes mainly occurred in communication with macrophages and was significantly reduced in IDD (Figure 6C). Therefore, the reduction of CXCL signaling in monocytes and macrophages may exacerbate the progression of IDD.

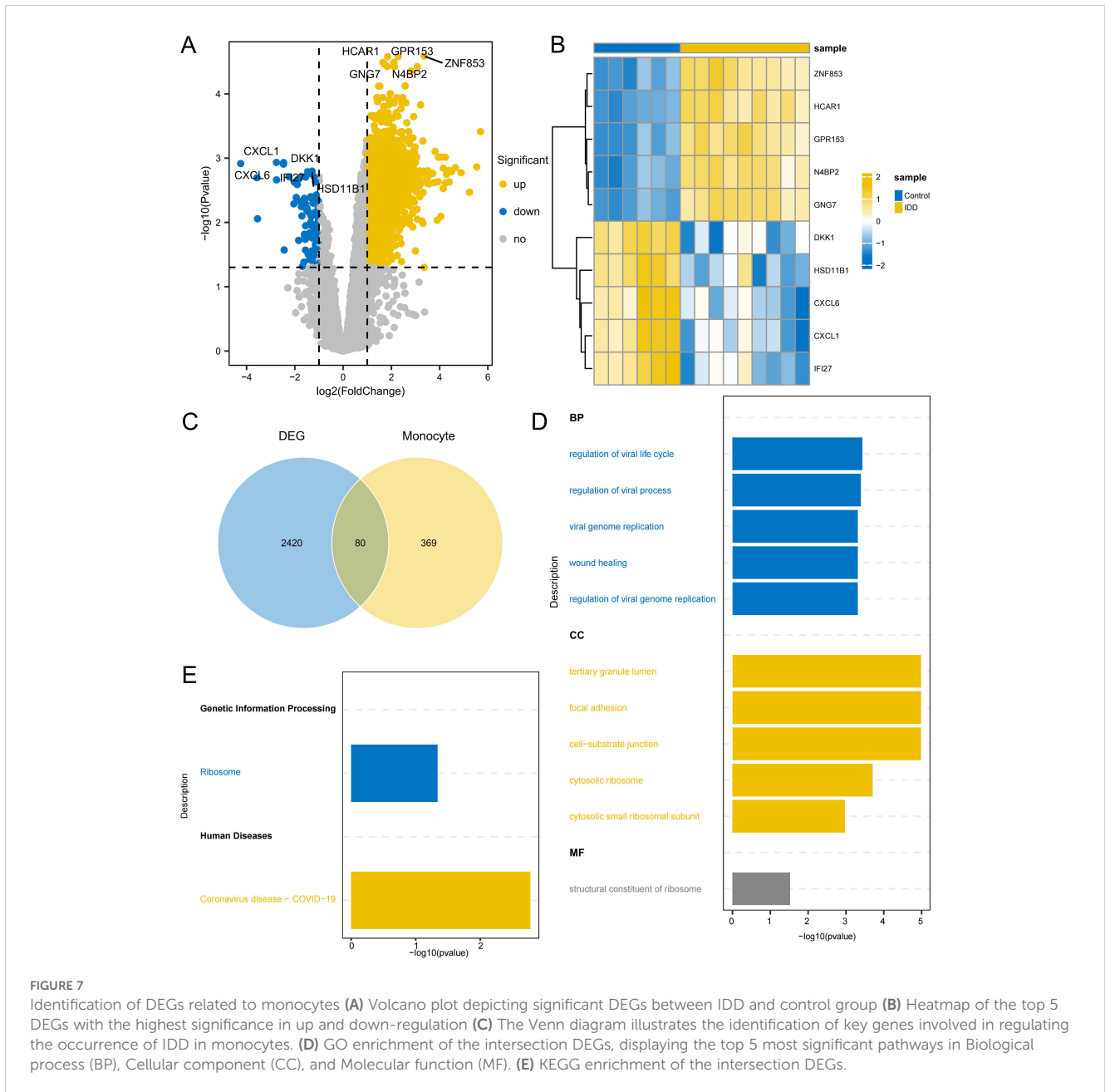
3.5 Identification of DEGs between IDD and control samples

2,500 DEGs were identified between IDD and control group, including 2,413 up-regulated genes and 87 down-regulated genes (Figures 7A, B; Supplementary Table 6). By intersecting DEGs from the conventional transcriptome with DEGs from monocytes, 80 intersecting DEGs were identified as key genes (Figure 7C; Supplementary Table 7). GO enrichment analysis indicated that these genes play significant roles in BPs, such as regulation of the

viral life cycle, regulation of viral processes, and viral genome replication. Additionally, CC, like tertiary granule lumen, focal adhesion, and cell-substrate junction, were enriched, as well as MF, such as the structural constituent of the ribosome (Figure 7D). KEGG analysis showed they were significantly enriched in Ribosome and Coronavirus disease - COVID-19 (Figure 7E; Supplementary Table 8). This suggests that ribosomes may be indirectly involved in the regulation of degenerative inflammatory responses by supporting the protein synthesis function of monocytes. The inflammatory environment of IDD activates monocytes, which synthesize and secrete a variety of inflammatory factors and degrading enzymes with the help of ribosomes, accelerating the destruction and degeneration of the intervertebral disc. Enrichment in viral biology suggests a role for the activation of inflammatory stress pathways in viral infection-mediated monocytes in IDD progression. Certain viruses, such as herpes simplex virus, can infect disc cells, causing direct cytopathy, inflammation, or apoptosis, which can accelerate disc degeneration (39). Coronavirus may also have a similar effect on disc degeneration.

3.6 Screening and validation of key genes

A PPI network was created for the intersecting DEGs using the STRING online database. The top 100 proteins in terms of importance were screened using 10 algorithms, including Betweenness, BottleNeck, Closeness, Degree, EcCentricity, EPC, MCC, MNC, Radiality, and Stress.



Six genes were identified through the intersection of these algorithms: POLR2A, RPLP0, JUN, CAT, IRF7, and RPS3 (Figure 8A). POLR2A, CAT, and IRF7 were included in the list of intersected DEGs, and RPLP0, JUN, and RPS3 were the genes that had a direct reciprocal relationship with the intersected DEGs. POLR2A, CAT, and IRF7 were selected as key genes for subsequent analysis. These essential genes showed up-regulation in the IDD group (Figure 8B). The ROC curves demonstrated POLR2A, CAT, and IRF7 all showed good efficacy for distinguishing IDD and standard samples (Figures 8C–E). Furthermore, the expression levels of these pivotal genes were confirmed in GSE167931. IRF7 were also significantly up-regulated. The expression of CAT in the IDD group is slightly upregulated, consistent with the trend in our analysis, which also shows potential as an IDD biomarker (Figure 8F). IRF7 showed promising efficacy for IDD and standard samples (AUC=0.9, Figure 8G).

3.7 Signaling pathways of key genes

GSEA showed the differences between the IDD and control groups across 50 Hallmark signaling pathways (Supplementary Table 9). In the IDD group, 3 pathways showed significant up-regulation and 15 pathways showed significant down-regulation (Figure 9A). IRF7 exhibits a significant negative correlation with HALLMARK_KRAS_SIGNALING_UP_PATHWAY, and down-regulation of HALLMARK_KRAS_SIGNALING_UP_PATHWAY has also been observed in IDD, suggesting that IRF7’s promotion of IDD may be mediated by inhibition of the KRAS pathway (Figure 9B). The activation of KRAS can upregulate the expression of the anti-apoptotic protein Bcl-2, thereby inhibiting apoptosis (40). In IDD, KRAS may be inhibited, leading to increased apoptosis of NPCs.

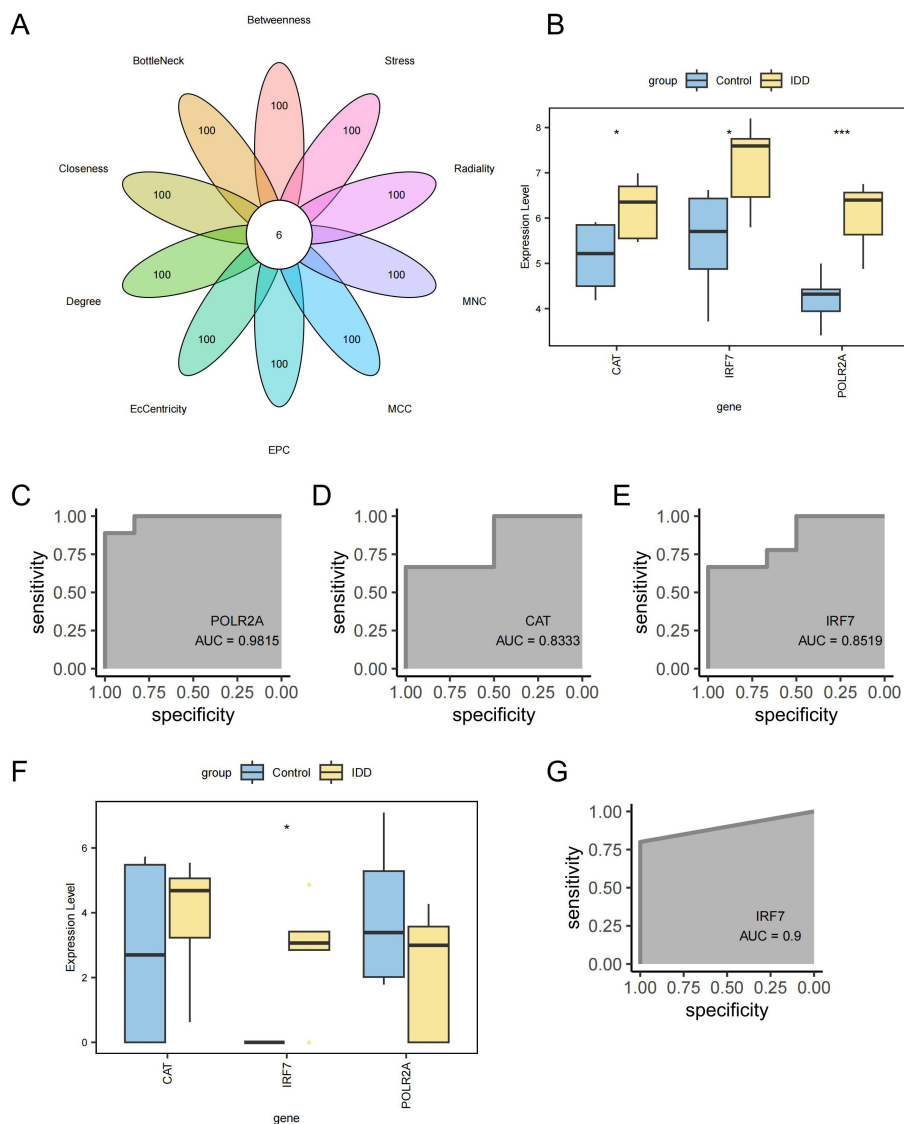


FIGURE 8 Screening of key Genes. **(A)** Six genes were identified through a combination of 10 network topology algorithms. **(B)** Key genes were significantly up-regulated in the IDD group. **(C)** ROC curve for gene POLR2A. **(D)** ROC curve for gene CAT. **(E)** ROC curve for gene IRF7. **(F)** Box plot showing differential expression of key genes in the external validation cohort GSE167931. **(G)** ROC curve for gene IRF7 in the external validation cohort GSE167931. ***p < 0.001, *p < 0.05.

3.8 Construction of key gene co-expression networks

To delve deeper into the function of the key genes, a co-expression network was constructed utilizing the GeneMANIA database (Figure 10A; Supplementary Table 10). The correlation heatmap between hub genes is shown in Figure 10B, demonstrating that most key genes were closely correlated with each other. GO and KEGG enrichment analysis found that it is related to lipid metabolism and peroxide pathways. This suggests that three hub genes and closely interacting genes may be involved in IDD progression by mediating these processes (Figures 10C, D; Supplementary Table 11). Specifically, lipid metabolism disorders can lead to abnormal deposition of lipids in the intervertebral discs, triggering an inflammatory response (41). Lipid peroxidation accelerates disc cell damage and matrix degradation by

increasing oxidative stress and promoting an inflammatory response (42). These processes interact with each other to form a vicious circle that ultimately leads to the progression of disc degeneration.

3.9 Correlation network construction of key genes

In order to further study the way of hub gene regulation, we constructed mRNA, TF, and ceRNA regulatory networks. An mRNA-miRNA-lncRNA interaction network was constructed using the key genes. Two miRNAs (miR-30a-5p and miR-30b-5p) were found to bind to CAT. A total of 23 lncRNAs were identified as target lncRNAs. The ceRNA network is shown in Figure 11A (Supplementary Table 12). The corresponding mRNA/RBP pairs

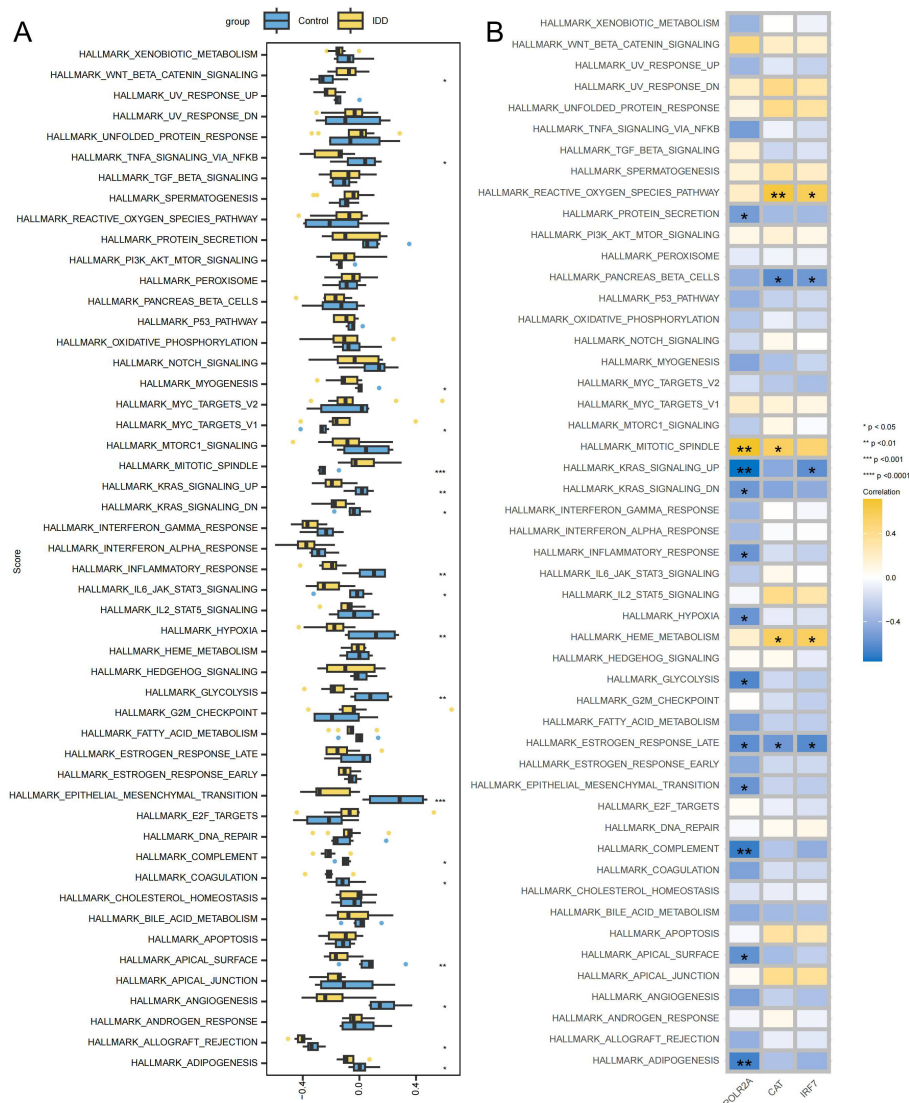


FIGURE 9 Signaling pathways associated with key genes (A) Box plot displaying differentially enriched pathways between the IDD and the control group. (B) Correlation between key genes and signaling pathways, with yellow indicating positive correlations and blue indicating negative correlations. ***p < 0.001, **p < 0.01, *p < 0.05.

of hub mRNAs with pairwise information were searched and downloaded using the StarBase online database. Based on the relationships identified among the target genes from the online dataset, we constructed an intricate RBP-mRNA network (Figure 11B; Supplementary Table 13). Transcription factors (TFs) that bind to co-expressed genes were searched using the TRRUST database, identifying interaction relationship data for 2 target genes and 17 TFs (Figure 11C; Supplementary Table 14).

3.10 Differential expression of IRF7 was the most significant, and knockdown of IRF7 alleviated IDD in NPCs

Using RT-qPCR analysis, it was noted that IRF7, POLR2A, and CAT exhibited significant upregulation in the TBHP-induced

degeneration group, with IRF7 showing the most significant increase in expression (Supplementary Figure 1). IDD can cause an imbalance between catabolism and anabolism in the ECM, leading to structural changes in the intervertebral disk (43). To investigate the potential of knocking down IRF7 to reverse IDD *in vitro*, we set up four groups of experiments: standard group, IDD group (TBHP), Si-NC group (TBHP + Si-NC), and Si-IRF7 group (TBHP + Si-IRF7). The efficiency of the IRF7 knockdown in NPCs was verified by RT-qPCR (Supplementary Figure 1). It was found that knocking down IRF7 increased the expression of COL2A1 in the Si-IRF7 group while decreasing the expression of MMP13 compared to the Si-NC group (Figures 12A, B, E). It indicates that the knockdown of IRF7 can reverse the metabolic imbalance of the extracellular matrix (ECM). Besides, the knockdown of IRF7 decreased the expression of NLRP3 and IL-1 β compared to the Si-NC group (Figures 12C-E). This indicates that knocking down

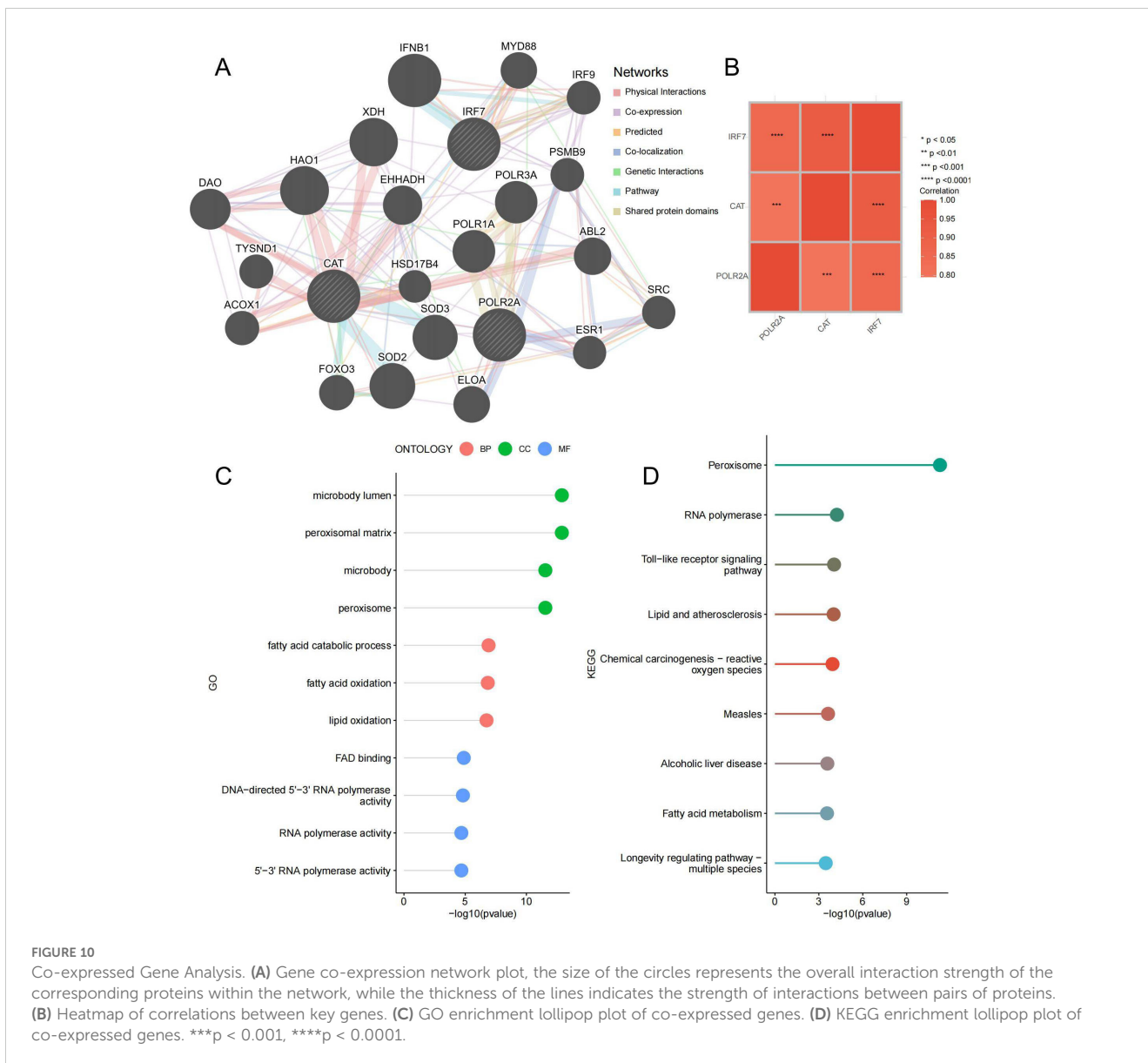


FIGURE 10

Co-expressed Gene Analysis. (A) Gene co-expression network plot, the size of the circles represents the overall interaction strength of the corresponding proteins within the network, while the thickness of the lines indicates the strength of interactions between pairs of proteins. (B) Heatmap of correlations between key genes. (C) GO enrichment lollipop plot of co-expressed genes. (D) KEGG enrichment lollipop plot of co-expressed genes. ***p < 0.001, ****p < 0.0001.

IRF7 can alleviate the inflammation of IDD. In conclusion, these findings demonstrate that the knockdown of IRF7 can slow the progression of NPC degeneration.

3.11 *In vivo* therapeutic effects of knocking down IRF7 in a rat model of IDD

Finally, we investigated the potential of knocking down IRF7 to reverse IDD *in vivo*. The flowchart of the animal experiment is shown in Figure 13A. Immunohistochemistry showed higher IRF7 expression in the Si-NC group than in the control group, and IRF7 was successfully knocked down *in vivo* (Supplementary Figure 2). 4 weeks after the knockdown of IRF7, X-ray analysis showed an increased intervertebral space height in the Si-IRF7 group compared to the Si-NC group, with corresponding increases in DHI scores

(Figures 13B, C). MRI results indicated significantly higher signal intensity in the Si-IRF7 group than in the Si-NC group, consistent with the grading results (Figures 13D, E). Both X-ray and MRI analyses confirmed that the knockdown of IRF7 alleviated IDD. Histological analysis further validated the therapeutic effects of IRF7 knockdown. It was found that NPs in the Si-NC group gradually shrank with blurred borders and were replaced by AF contents. In contrast, the NPs in the Si-IRF7 group showed significantly restored morphology (Figure 13F). The expression of COL2A1, MMP13, NLRP3 and IL-1 β in NP tissues was accessed with immunohistochemical staining. The knockdown of IRF7 significantly restored the expression of COL2A1, while the expression of MMP13, NLRP3 and IL-1 β was significantly reduced (Figure 14). These findings collectively demonstrate that the knockdown of IRF7 can inhibit inflammation and reverse the metabolic imbalance of the ECM, thereby alleviating the progression of IDD.

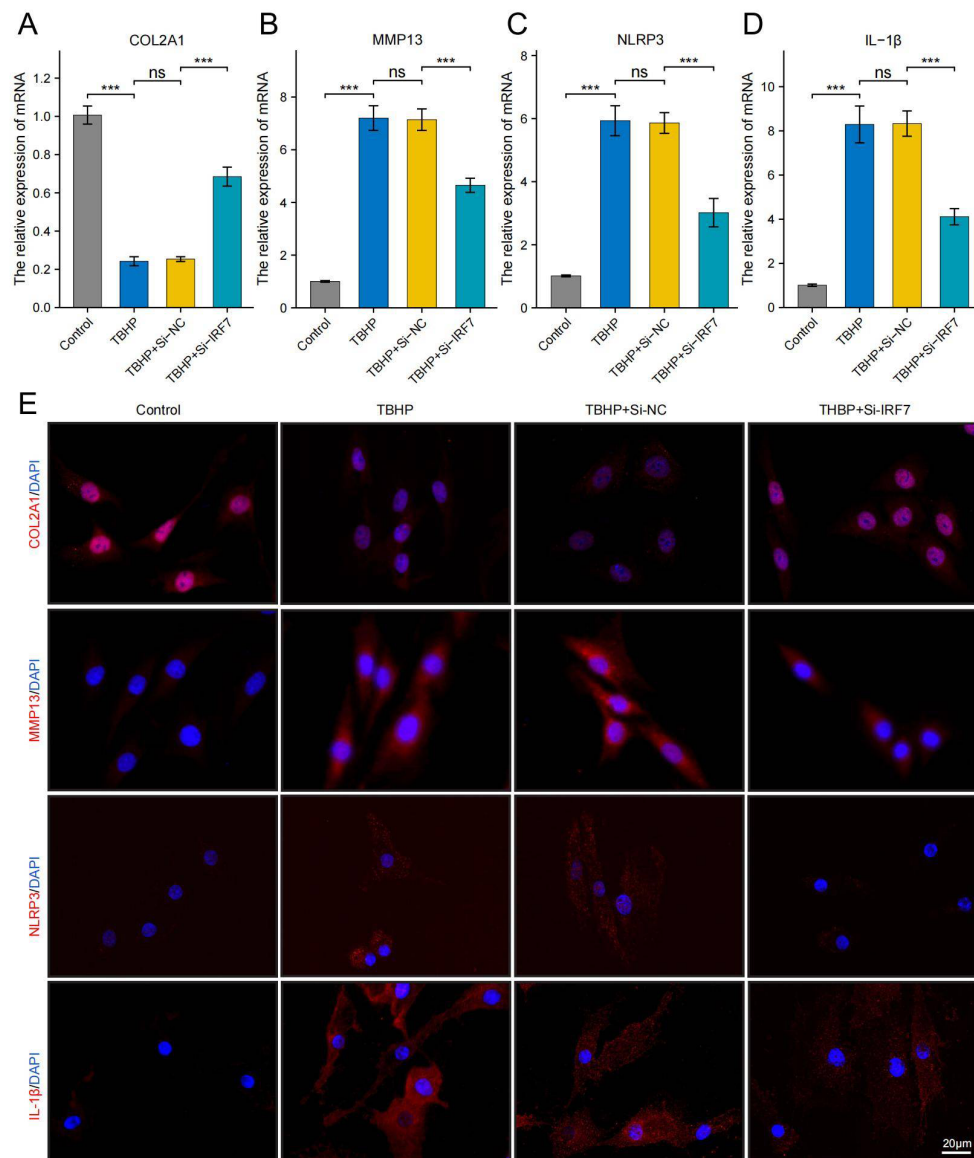


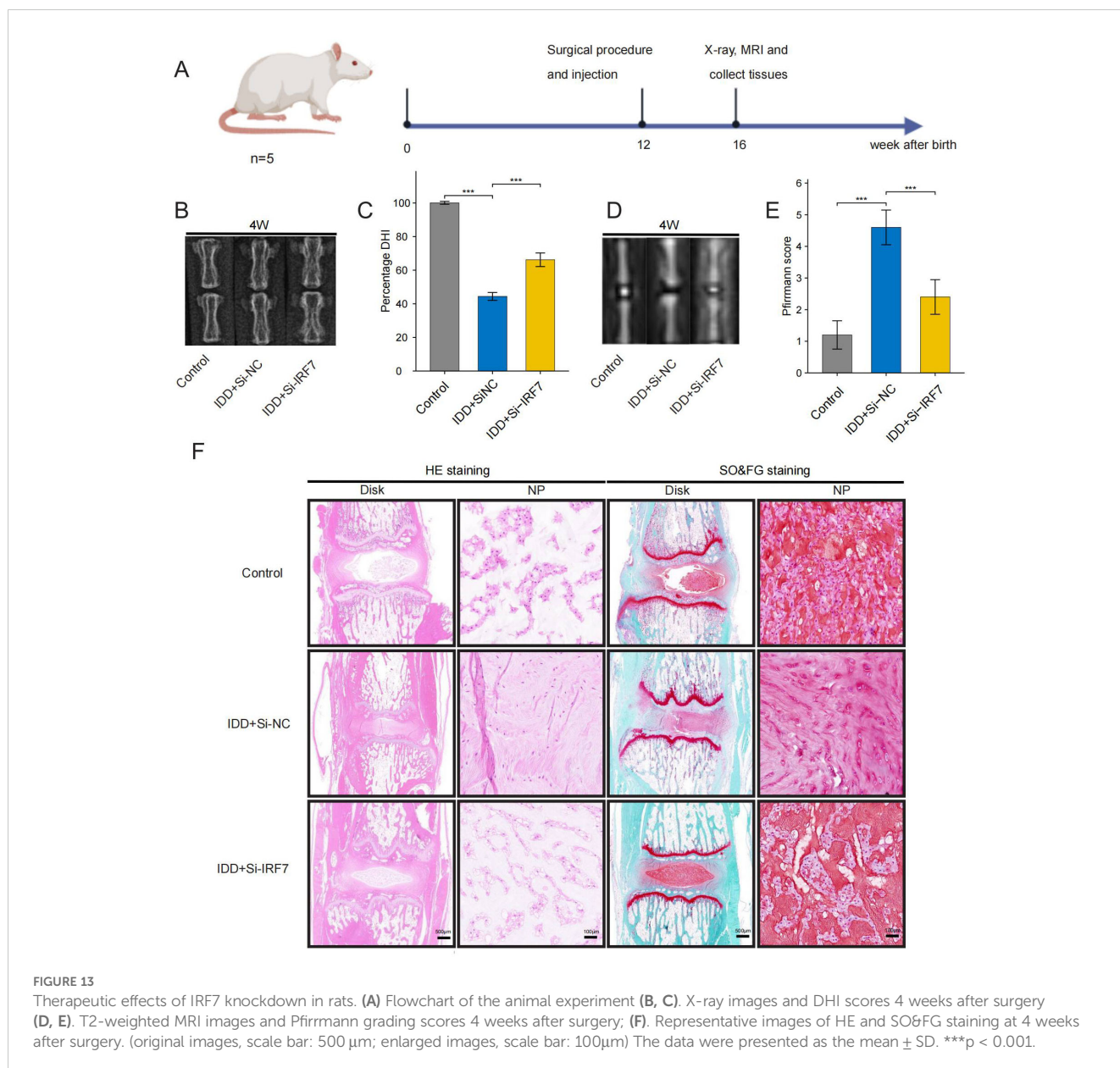
FIGURE 12 Knockdown of the IRF7 gene can alleviate the degeneration of NPCs. (A–D) RT-qPCR shows changes in COL2A1, MMP13, NLRP3 and IL-1β expression levels. (E) Immunofluorescence shows changes in COL2A1, MMP13, NLRP3 and IL-1β expression levels.(scale bar: 20μm) The data were presented as the mean ± SD. ***p < 0.001.

promoting intervertebral disc repair. These emerging therapies are expected to provide patients with IDD with more effective and lasting solutions to reduce LBP symptoms and improve quality of life.

Monocytes are a type of blood cell originating from bone marrow precursors and associated with the mononuclear phagocytic cell system (48). Monocytes are the second-line defense cells of the innate immune system after neutrophils and can engulf foreign particles. They can differentiate into their subpopulations and macrophages depending on the necessities of the microenvironment. In addition, monocytes produce cytokines and act as antigen-presenting cells (APCs) (49). In this study, machine-learning techniques were used to screen for immune cells, identifying monocytes as key players in the development and progression of IDD. Consistent with our findings, Guo et al. found through bioinformatics analysis that monocytes

infiltration was more frequent in the IDD group compared to the healthy group (50). Inflammation is a crucial factor in IDD progression, and IL-17 has been shown to recruit monocytes and neutrophils to sites of inflammation by increasing chemokine production (43). It can further amplify the inflammatory cascade, promote the degradation of the ECM, and accelerate the progression of IDD. As immune cells, monocytes initiate the defense against inflammation upon recruitment to inflammation sites under the chemotaxis of cytokines (51). A recent study also found that monocytes are abnormally activated in the late stages of IDD (52). Therefore, monocytes may play a pivotal role in the progression of IDD, leading to increased inflammation within the intervertebral disc.

The interaction of cytokines with intervertebral disc cells is one of the crucial mechanisms of IDD. NPCs undergo a series of biological



responses stimulated by cytokines, including apoptosis, proliferation, and matrix degradation (53). For example, IL-1β and TNF-α can promote the secretion of more inflammatory factors and matrix-degrading enzymes from NP and AF cells by activating the NF-κB and MAPK signaling pathways, thus forming a vicious circle and accelerating IDD (54). These cytokines promote the inflammatory response and lead to the degradation of the ECM by regulating the expression of enzymes such as matrix metalloproteinases (MMPs) and ADAMTS, thus accelerating IDD (55). In addition, it has been found that specific anti-inflammatory cytokines, such as IL-10, are expressed at low levels in intervertebral disc tissues, which may contribute to uncontrolled inflammation and increased degeneration (56). To systematically elucidate the effects of cytokines on monocytes in IDD, the present study identified an important role of type I interferon (IFN-α1, IFN-β) in the monocytes by IREA analysis. Type I interferons play a crucial role in antiviral immunity and influence inflammatory response and tissue repair by modulating the function of

multiple immune cells. They regulate the innate immune response by promoting antigen presentation and natural killer cell function (57). Besides, they can modulate inflammation by affecting key factors in various signaling pathways such as the JAK/STAT pathway, TLRs pathway, NF-κB pathway, PI3K/AKT pathway, and MAPK pathway (58). Secondly, IFN-Is can trigger the adaptive immune system and promote the development of high-affinity antigenic immune cell responses and immune memory (59, 60). During disc degeneration, monocytes may increase type I interferons, causing monocytes mono-polarization, increasing oxidative stress and promoting inflammatory responses to accelerate disc cell damage and matrix degradation.

Cell-cell communication analysis in IDD revealed that the ANNEXIN pathway was inhibited in the IDD group. Annexins were described as Ca²⁺-regulated membrane-binding modules that respond to cellular stress and control mammal inflammatory responses (61). Annexins have been proven to play an anti-inflammatory role in various diseases. Jia et al. found that Annexin A5 inhibited the release

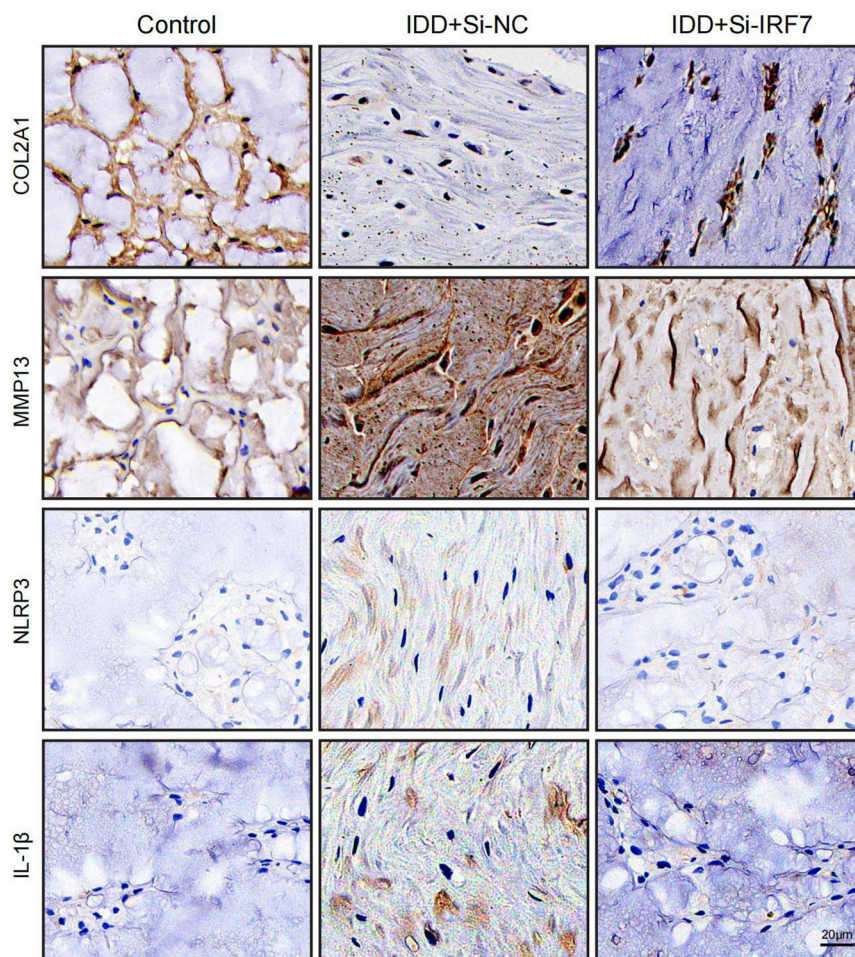


FIGURE 14 Representative images of immunohistochemistry at 4 weeks after surgery (scale bar: 20μm).

of pro-inflammatory mediators *in vitro* and reduced the production of reactive oxygen species in osteoarthritis, which protected chondrocyte necrosis and apoptosis (62). Similarly, You et al. found that Annexin A5 depletion exacerbates vascular remodelling and dysfunction while upregulating the expression of age- and inflammation-related proteins (63). Thus, the inhibition of the ANNEXIN pathway in IDD may prevent it from responding adequately to inflammatory stimuli in the intervertebral disc, contributing to the progression of IDD. As a member of the Annexin family, Annexin A1 exerts anti-inflammatory and pro-catabolic effects in various ways (64). In our study, we also found that the ligand ANXA1 showed a downward trend in all cell types in IDD, which may lead to a decrease in the anti-inflammatory effect of the IDD group. Michael Scannell found that AnxA1 can induce monocytes recruitment and enhance phagocytosis, confirming our conjecture (65). Additionally, Shao et al. found that NPCs can seek the help of neutrophils through the ANXA1-FPR1 pathway to alleviate intervertebral disc inflammation (66). Our study found that the receptor FPR1 expression was highest among monocytes. Therefore, the ANXA1-FPR1 pathway may alleviate inflammation in the intervertebral disc by recruiting monocytes.

Subsequently, we intersected the genes specifically expressed in monocytes from the single-cell data with the DEGs between IDD

and healthy controls from the transcriptome. The core genes POLR2A, CAT, and IRF7 were identified using ten algorithms. The differential expression of CAT and IRF7 was validated in an external dataset, GSE167931, further confirming their central roles in IDD development. Similar results were obtained from *in vitro* experiments, where significantly higher expression of POLR2A, CAT, and IRF7 was observed in TBHP-induced IDD samples, verifying the reliability of our analysis.

RNA polymerase II subunit A (POLR2A) is the largest subunit encoding RNA polymerase II, which plays a crucial role in transcription. Although no literature directly supports its relationship with IDD, external validation has demonstrated high expression of POLR2A in the IDD group. GSVA supported the significant correlation between POLR2A and numerous Hallmark pathways enriched in the IDD group, indicating that abnormalities in POLR2A can lead to changes in multiple pathways, such as HALLMARK_MITOTIC_SPINDLE and HALLMARK_KARS_SIGNALING_UP, thereby affecting IDD progression. CAT encodes catalase, a critical antioxidant enzyme that protects cells from oxidative damage. Xiang et al. found that Nrf2 signaling promotes the transcription of downstream antioxidant genes, including CAT, which in turn come to protect against oxidative

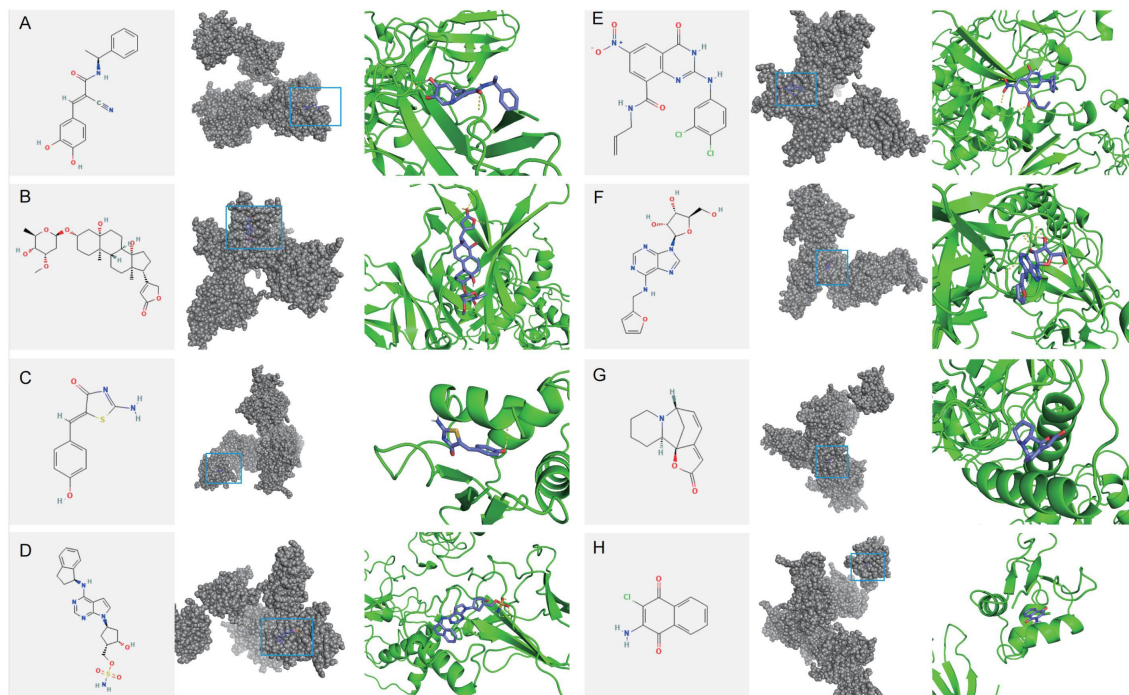


FIGURE 15

Molecular docking of potential drug molecules with their corresponding target proteins. (A) Tyrphostin AG 835 (B) Periplocymarin (C) Mirin (D) MLN-4924 (E) AZ-10417808 (F) Kinetin riboside (G) Securinine (H) Quinoclamine.

stress in intervertebral disc cells (67). Xiao et al. found that CAT could significantly reduce oxidative stress in intervertebral disc cells, thereby reducing apoptosis and inflammation and slowing down disc degeneration (68). GSVA analysis also showed that CAT was associated with HALLMARK_REACTIVE_OXYGEN_SPECIES_PATHWAY, further supporting its protective role in oxidative stress regulation. Thus, CAT may slow the progression of IDD by acting on the process of oxidative stress.

Interferon regulatory factor 7 (IRF7), a member of the IRF family, is a crucial regulator of type I interferon production (69). IRF7 can form a positive feedback loop with IFN-Is, significantly enhancing their expression and maintaining high levels of IFN-Is, thus actively regulating IFN-I production (70, 71). Koroth et al. found that interferons can play a crucial role in disc degeneration by modulating macrophage polarisation and influencing the inflammatory response of disc cells (72). Several studies have shown that IRF7 regulates inflammation in various diseases, however, its role in IDD remains unelucidated. Chen et al. demonstrated that IRF7 can promote apoptosis of intestinal epithelial cells and the release of pro-inflammatory proteins by activating the Nod-like receptor (NLR) pathway, thereby exacerbating intestinal inflammation (73). He et al. found that ILC2 from asthmatics exhibited much higher levels of IRF7 than healthy donors upon stimulation with papain or IL-33, suggesting that IRF7 may promote the development of asthma (74). Moreover, Aryl Hydrocarbon Receptor Interacting Protein (AIP) can inhibit IRF7 by antagonizing its nuclear localization, hindering IRF7-induced IFN-I production, reducing immune responses, and promoting aberrant inflammation (75). In this study, IRF7 was identified as a critical gene for IDD through PPI network analysis

and was significantly up-regulated in IDD samples. *In vitro*, it was found that knocking down IRF7 can slow the progression of IDD. Compared with the Si-NC group, the expression levels of COL2A1 increased, while the expression level of MMP13, NLRP3 and IL-1 β decreased after IRF7 knockdown. Subsequently, an IDD model in rats was constructed to verify the function of IRF7 further. X-ray showed that the intervertebral disc height in the Si-IRF7 group was higher than in the Si-NC group. MRI revealed that the water content of the intervertebral disc in the Si-IRF7 group was also higher than in the Si-NC group. HE and SF staining demonstrated that the morphology of the NP in the Si-IRF7 group was better restored than in the Si-NC group. Finally, immunohistochemistry confirmed that knocking down IRF7 can delay the progression of IDD by regulating inflammation and the metabolism of the extracellular matrix. Therefore, this study demonstrates through *in vivo* and *in vitro* experiments that IRF7 is an essential therapeutic target for IDD, and knocking down IRF7 can significantly alleviate IDD.

Eight small-molecule drugs were then screened that may alleviate IDD: Tyrphostin-AG-835, Periplocymarin, Mirin, MLN-4924, AZ-10417808, Kinetin-riboside, Securinine, and Quinoclamine. Molecular docking showed that IRF7 tightly binds to these potential small-molecule drugs, suggesting they may exert therapeutic effects by binding to IRF7 in IDD.

However, this study is subject to certain constraints. Firstly, the crucial role of monocytes and IRF7 in IDD has been demonstrated, but the specific mechanisms of action remain to be further investigated. Additionally, conducting *in vitro* drug tests and clinical trials is crucial to confirm the therapeutic effect of these small-molecule drugs on the progression of IDD.

5 Conclusion

Monocytes are essential in the progression of IDD, with the polarisation state of monocytes mediated by type I interferon potentially exacerbating the inflammatory response in the intervertebral disc. IRF7 has been identified as a key target for IDD, and its role in causing IDD has been confirmed through both *in vitro* and *in vivo* studies. These studies provide novel insights into potential therapeutic targets for IDD. Future research should encompass more extensive clinical sample analyses to confirm these discoveries and facilitate their translation into clinical applications.

Data availability statement

The original contributions presented in the study are included in the article/[Supplementary Material](#). Further inquiries can be directed to the corresponding author.

Ethics statement

The animal study was approved by the Animal Ethics Committee of Nanchang University. The study was conducted in accordance with the local legislation and institutional requirements.

Author contributions

PX: Writing – review & editing, Writing – original draft, Supervision, Software, Conceptualization. KL: Writing – review & editing, Investigation, Writing – original draft, Validation. JY: Writing – review & editing, Software, Methodology, Formal analysis. JZ: Writing – review & editing, Validation, Methodology, Writing – original draft. HP: Writing – original draft, Validation. CP: Validation, Writing – original draft, Methodology. WX: Supervision, Writing – review & editing. JT: Writing – review & editing, Investigation. TL: Writing – review & editing, Methodology. GH: Software, Formal analysis, Writing – original draft. XLC: Software, Formal analysis, Writing – original draft. XM: Writing – review & editing, Methodology. DH: Writing – review & editing, Supervision. XGC: Writing – review & editing, Supervision, Project administration, Funding acquisition, Conceptualization.

Funding

The author(s) declare financial support was received for the research, authorship, and/or publication of this article. This research was funded by the National Natural Science Foundation of China (Grant Number:82060403) and International Scientific and Technological Cooperation Project (Grant Number:20232BBH80001).

Conflict of interest

The authors declare that the research was conducted in the absence of any commercial or financial relationships that could be construed as a potential conflict of interest.

Publisher's note

All claims expressed in this article are solely those of the authors and do not necessarily represent those of their affiliated organizations, or those of the publisher, the editors and the reviewers. Any product that may be evaluated in this article, or claim that may be made by its manufacturer, is not guaranteed or endorsed by the publisher.

Supplementary material

The Supplementary Material for this article can be found online at: <https://www.frontiersin.org/articles/10.3389/fimmu.2024.1465126/full#supplementary-material>

SUPPLEMENTARY TABLE 1
Primers used in this study.

SUPPLEMENTARY TABLE 2
The result of ssGSEA.

SUPPLEMENTARY TABLE 3
DEGs in monocytes of IDD and Control groups.

SUPPLEMENTARY TABLE 4
The result of IREA(cytokines).

SUPPLEMENTARY TABLE 5
The result of IREA(cell polarisation).

SUPPLEMENTARY TABLE 6
2500 DEGs between IDD and control groups.

SUPPLEMENTARY TABLE 7
Intersecting 80 DEGs.

SUPPLEMENTARY TABLE 8
The results of the GO and KEGG enrichment analysis.

SUPPLEMENTARY TABLE 9
The results of GSVA.

SUPPLEMENTARY TABLE 10
The co-expression network of key genes.

SUPPLEMENTARY TABLE 11
GO and KEGG enrichment of 23 genes.

SUPPLEMENTARY TABLE 12
The results of the ceRNA network.

SUPPLEMENTARY TABLE 13
The results of the RBP network.

SUPPLEMENTARY TABLE 14
The results of the TF network.

SUPPLEMENTARY TABLE 15
The results of small-molecule drug prediction..

SUPPLEMENTARY FIGURE 1
Differential expression of three hub genes and IRF7 was knocked down *in vitro*.

SUPPLEMENTARY FIGURE 2
IRF7 was successfully knocked down *in vivo*.

References

- Wei B, Zhao Y, Li W, Zhang S, Yan M, Hu Z, et al. Innovative immune mechanisms and antioxidative therapies of intervertebral disc degeneration. *Front Bioengineering Biotechnol.* (2022) 10:1023877. doi: 10.3389/fbioe.2022.1023877
- Zhou D, Mei Y, Song C, Cheng K, Cai W, Guo D, et al. Exploration of the mode of death and potential death mechanisms of nucleus pulposus cells. *Eur J Clin Invest.* (2024) 54:e14226. doi: 10.1111/eci.14226
- Li S, Du J, Huang Y, Gao S, Zhao Z, Chang Z, et al. From hyperglycemia to intervertebral disc damage: exploring diabetic-induced disc degeneration. *Front Immunol.* (2024) 15:1355503. doi: 10.3389/fimmu.2024.1355503
- Swahn H, Mertens J, Olmer M, Myers K, Mondala TS, Natarajan P, et al. Shared and compartment-specific processes in nucleus pulposus and annulus fibrosus during intervertebral disc degeneration. *Advanced Sci (Weinheim Baden-Wuerttemberg Germany).* (2024) 11:e2309032. doi: 10.1002/adv.202309032
- Minamisawa Y, Shirogane T, Watanabe I, Dezawa A. Histological analysis of nucleus pulposus tissue from patients with lumbar disc herniation after condoliase administration. *JOR Spine.* (2024) 7:e1328. doi: 10.1002/jsp.21328
- Lu J, Tian Z, Shofar FS, Qin L, Sun H, Zhang Y. Tnfrsf8 and tpe2 gene deletion ameliorates immediate proteoglycan loss and inflammatory responses in the injured mouse intervertebral disc. *Am J Phys Med Rehabil.* (2024) 103:918–24. doi: 10.1097/PHM.0000000000002488
- Song C, Hu P, Peng R, Li F, Fang Z, Xu Y. Bioenergetic dysfunction in the pathogenesis of intervertebral disc degeneration. *Pharmacol Res.* (2024) 202:107119. doi: 10.1016/j.phrs.2024.107119
- Li Y, Liu S, Pan D, Xu B, Xing X, Zhou H, et al. The potential role and trend of HIF-1 α in intervertebral disc degeneration: Friend or foe? (Review). *Mol Med Rep.* (2021) 23:239. doi: 10.3892/mmr.2021.11878
- Sun Z, Liu B, Luo ZJ. The immune privilege of the intervertebral disc: implications for intervertebral disc degeneration treatment. *Int J Med Sci.* (2020) 17:685–92. doi: 10.15170/ijms.42238
- Capossela S, Schläfli P, Bertolo A, Janner T, Stadler BM, Pötzel T, et al. Degenerated human intervertebral discs contain autoantibodies against extracellular matrix proteins. *Eur Cells Materials.* (2014) 27:251–63. doi: 10.22023/eCM.v027a18
- Vergroesen PP, Kingma I, Emanuel KS, Hoogendoorn RJ, Welting TJ, van Royen BJ, et al. Mechanics and biology in intervertebral disc degeneration: a vicious circle. *Osteoarthritis Cartilage.* (2015) 23:1057–70. doi: 10.1016/j.joca.2015.03.028
- Arai KI, Lee F, Miyajima A, Miyatake S, Arai N, Yokota T. Cytokines: coordinators of immune and inflammatory responses. *Annu Rev Biochem.* (1990) 59:783–836. doi: 10.1146/annurev.bi.59.070190.004031
- Briukhovetska D, Dörr J, Endres S, Libby P, Dinarello CA, Kobold S. Interleukins in cancer: from biology to therapy. *Nat Rev Cancer.* (2021) 21:481–99. doi: 10.1038/s41568-021-00363-z
- Le Maitre CL, Freemont AJ, Hoyland JA. The role of interleukin-1 in the pathogenesis of human intervertebral disc degeneration. *Arthritis Res Ther.* (2005) 7:R732–45. doi: 10.1186/ar1732
- Hoyland JA, Le Maitre C, Freemont AJ. Investigation of the role of IL-1 and TNF in matrix degradation in the intervertebral disc. *Rheumatol (Oxford England).* (2008) 47:809–14. doi: 10.1093/rheumatology/ken056
- Phillips KL, Chiverton N, Michael AL, Cole AA, Breakwell LM, Haddock G, et al. The cytokine and chemokine expression profile of nucleus pulposus cells: implications for degeneration and regeneration of the intervertebral disc. *Arthritis Res Ther.* (2013) 15:R213. doi: 10.1186/ar4408
- Phillips KL, Cullen K, Chiverton N, Michael AL, Cole AA, Breakwell LM, et al. Potential roles of cytokines and chemokines in human intervertebral disc degeneration: interleukin-1 is a master regulator of catabolic processes. *Osteoarthritis Cartilage.* (2015) 23:1165–77. doi: 10.1016/j.joca.2015.02.017
- Li S, Pan X, Wu Y, Tu Y, Hong W, Ren J, et al. IL-37 alleviates intervertebral disc degeneration via the IL-1R8/NF- κ B pathway. *Osteoarthritis Cartilage.* (2023) 31:588–99. doi: 10.1016/j.joca.2023.01.006
- Tian Y, Chu X, Huang Q, Guo X, Xue Y, Deng W. Astragaloside IV attenuates IL-1 β -induced intervertebral disc degeneration through inhibition of the NF- κ B pathway. *J Orthopaedic Surg Res.* (2022) 17:545. doi: 10.1186/s13018-022-03438-1
- Purmessur D, Freemont AJ, Hoyland JA. Expression and regulation of neurotrophins in the nondegenerate and degenerate human intervertebral disc. *Arthritis Res Ther.* (2008) 10:R99. doi: 10.1186/ar2487
- Binch AL, Cole AA, Breakwell LM, Michael AL, Chiverton N, Cross AK, et al. Expression and regulation of neurotrophic and angiogenic factors during human intervertebral disc degeneration. *Arthritis Res Ther.* (2014) 16:416. doi: 10.1186/s13075-014-0416-1
- Saxton RA, Glassman CR, Garcia KC. Emerging principles of cytokine pharmacology and therapeutics. *Nat Rev Drug Discovery.* (2023) 22:21–37. doi: 10.1038/s41573-022-00557-6
- Leek JT, Johnson WE, Parker HS, Jaffe AE, Storey JD. The sva package for removing batch effects and other unwanted variation in high-throughput experiments. *Bioinf (Oxford England).* (2012) 28:882–3. doi: 10.1093/bioinformatics/bts034
- Butler A, Hoffman P, Smibert P, Papalexi E, Satija R. Integrating single-cell transcriptomic data across different conditions, technologies, and species. *Nat Biotechnol.* (2018) 36:411–20. doi: 10.1038/nbt.4096
- Wu S, Lv X, Li Y, Gao X, Ma Z, Fu X, et al. Integrated machine learning and single-sample gene set enrichment analysis identifies a TGF- β signaling pathway derived score in headneck squamous cell carcinoma. *J Oncol.* (2022) 2022:3140263. doi: 10.1155/2022/3140263
- Cui A, Huang T, Li S, Ma A, Pérez JL, Sander C, et al. Dictionary of immune responses to cytokines at single-cell resolution. *Nature.* (2024) 625:377–84. doi: 10.1038/s41586-023-06816-9
- Fang Z, Tian Y, Sui C, Guo Y, Hu X, Lai Y, et al. Single-cell transcriptomics of proliferative phase endometrium: systems analysis of cell-cell communication network using cellChat. *Front Cell Dev Biol.* (2022) 10:919731. doi: 10.3389/fcell.2022.919731
- Ritchie ME, Phipson B, Wu D, Hu Y, Law CW, Shi W, et al. limma powers differential expression analyses for RNA-sequencing and microarray studies. *Nucleic Acids Res.* (2015) 43:e47. doi: 10.1093/nar/gkv007
- Szklarczyk D, Gable AL, Nastou KC, Lyon D, Kirsch R, Pyysalo S, et al. The STRING database in 2021: customizable protein-protein networks, and functional characterization of user-uploaded gene/measurement sets. *Nucleic Acids Res.* (2021) 49:D605–d612. doi: 10.1093/nar/gkaa1074
- Shannon P, Markiel A, Ozier O, Baliga NS, Wang JT, Ramage D, et al. Cytoscape: a software environment for integrated models of biomolecular interaction networks. *Genome Res.* (2003) 13:2498–504. doi: 10.1101/gr.1239303
- Blake JA, Christie KR, Dolan ME, Drabkin HJ, Hill DP, Ni L, et al. Gene Ontology Consortium: going forward. *Nucleic Acids Res.* (2015) 43:D1049–56. doi: 10.1093/nar/gku1179
- Kanehisa M, Goto S. KEGG: kyoto encyclopedia of genes and genomes. *Nucleic Acids Res.* (2000) 28:27–30. doi: 10.1093/nar/28.1.27
- Yu G, Wang LG, Han Y, He QY. clusterProfiler: an R package for comparing biological themes among gene clusters. *Omic: J Integr Biol.* (2012) 16:284–7. doi: 10.1089/omi.2011.0118
- Warde-Farley D, Donaldson SL, Comes O, Zuberi K, Badrawi R, Chao P, et al. The GeneMANIA prediction server: biological network integration for gene prioritization and predicting gene function. *Nucleic Acids Res.* (2010) 38:W214–20. doi: 10.1093/nar/gkq537
- Huang HY, Lin YC, Cui S, Huang Y, Tang Y, Xu J, et al. miRTarBase update 2022: an informative resource for experimentally validated miRNA-target interactions. *Nucleic Acids Res.* (2022) 50:D222–d230. doi: 10.1093/nar/gkab1079
- Li JH, Liu S, Zhou H, Qu LH, Yang JH. starBase v2.0: decoding miRNA-*ce*RNA, miRNA-*nc*RNA and protein-RNA interaction networks from large-scale CLIP-Seq data. *Nucleic Acids Res.* (2014) 42:D92–7. doi: 10.1093/nar/gkt1248
- Xiong L, Li X, Hua X, Qian Z. Circ-STC2 promotes the ferroptosis of nucleus pulposus cells via targeting miR-486-3p/TFR2 axis. *J Orthopaedic Surg Res.* (2023) 18:518. doi: 10.1186/s13018-023-04010-1
- Han B, Zhu K, Li FC, Xiao YX, Feng J, Shi ZL, et al. A simple disc degeneration model induced by percutaneous needle puncture in the rat tail. *Spine (Phila Pa 1976).* (2008) 33:1925–34. doi: 10.1097/BRS.0b013e31817c64a9
- Alpantaki K, Zafiroopoulos A, Tseliou M, Vasarmidi E, Sourvinos G. Herpes simplex virus type-1 infection affects the expression of extracellular matrix components in human nucleus pulposus cells. *Virus Res.* (2019) 259:10–7. doi: 10.1016/j.virusres.2018.10.010
- Tripathi PK, Mittal KR, Jain N, Sharma N, Jain CK. KRAS pathways: A potential gateway for cancer therapeutics and diagnostics. *Recent Patents Anti-Cancer Drug Discovery.* (2024) 19:268–79. doi: 10.2174/1574892818666230406085120
- Yi J, Zhou Q, Huang J, Niu S, Ji G, Zheng T. Lipid metabolism disorder promotes the development of intervertebral disc degeneration. *Biomedicine Pharmacotherapy = Biomedecine pharmacotherapie.* (2023) 166:115401. doi: 10.1016/j.biopha.2023.115401
- Dou X, Ma Y, Luo Q, Song C, Liu M, Liu X, et al. Therapeutic potential of melatonin in the intervertebral disc degeneration through inhibiting the ferroptosis of nucleus pulposus cells. *J Cell Mol Med.* (2023) 27:2340–53. doi: 10.1111/jcmm.v27.16
- Risbud MV, Shapiro IM. Role of cytokines in intervertebral disc degeneration: pain and disc content. *Nat Rev Rheumatol.* (2014) 10:44–56. doi: 10.1038/nrrheum.2013.160
- Taylor VM, Deyo RA, Cherkin DC, Kreuter W. Low back pain hospitalization. Recent United States trends and regional variations. *Spine.* (1994) 19:1207–12. doi: 10.1097/00007632-199405310-00002
- Andersson GB. Epidemiological features of chronic low-back pain. *Lancet (London England).* (1999) 354:581–5. doi: 10.1016/S0140-6736(99)01312-4
- Millemcamps M, Czerminski JT, Mathieu AP, Stone LS. Behavioral signs of axial low back pain and motor impairment correlate with the severity of intervertebral disc degeneration in a mouse model. *Spine Journal: Off J North Am Spine Soc.* (2015) 15:2524–37. doi: 10.1016/j.spinee.2015.08.055
- Bermudez-Lekerika P, Crump KB, Tseranidou S, Nüesch A, Kanelis E, Alminnawi A, et al. Immuno-modulatory effects of intervertebral disc cells. *Front Cell Dev Biol.* (2022) 10:924692. doi: 10.3389/fcell.2022.924692

48. Ziegler-Heitbrock L, Ancuta P, Crowe S, Dalod M, Grau V, Hart DN, et al. Nomenclature of monocytes and dendritic cells in blood. *Blood*. (2010) 116:e74–80. doi: 10.1182/blood-2010-02-258558
49. Liu EG, Yin X, Swaminathan A, Eisenbarth SC. Antigen-presenting cells in food tolerance and allergy. *Front Immunol*. (2020) 11:616020. doi: 10.3389/fimmu.2020.616020
50. Guo D, Zeng M, Yu M, Shang J, Lin J, Liu L, et al. SSR1 and CKAP4 as potential biomarkers for intervertebral disc degeneration based on integrated bioinformatics analysis. *JOR Spine*. (2024) 7:e1309. doi: 10.1002/jsp2.1309
51. Kratochvil RM, Kubes P, Deniset JF. Monocyte conversion during inflammation and injury. *Arteriosclerosis Thrombosis Vasc Biol*. (2017) 37:35–42. doi: 10.1161/ATVBAHA.116.308198
52. Li W, Zhao Y, Wang Y, He Z, Zhang L, Yuan B, et al. Deciphering the sequential changes of monocytes/macrophages in the progression of IDD with longitudinal approach using single-cell transcriptome. *Front Immunol*. (2023) 14:1090637. doi: 10.3389/fimmu.2023.1090637
53. Cabral VLF, Wang F, Peng X, Gao J, Zhou Z, Sun R, et al. Omeintin-1 promoted proliferation and ameliorated inflammation, apoptosis, and degeneration in human nucleus pulposus cells. *Arch Gerontology Geriatrics*. (2022) 102:104748. doi: 10.1016/j.archger.2022.104748
54. Kang H, Dong Y, Peng R, Liu H, Guo Q, Song K, et al. Inhibition of IRE1 suppresses the catabolic effect of IL-1 β on nucleus pulposus cell and prevents intervertebral disc degeneration *in vivo*. *Biochem Pharmacol*. (2022) 197:114932. doi: 10.1016/j.bcp.2022.114932
55. Liu W, Wang Y. Protective role of the alpha-1-antitrypsin in intervertebral disc degeneration. *J Orthopaedic Surg Res*. (2021) 16:516. doi: 10.1186/s13018-021-02668-z
56. Kim JH, Ham CH, Kwon WK. Current knowledge and future therapeutic prospects in symptomatic intervertebral disc degeneration. *Yonsei Med J*. (2022) 63:199–210. doi: 10.3349/ymj.2022.63.3.199
57. Meyer O. Interferons and autoimmune disorders. *Joint Bone Spine*. (2009) 76:464–73. doi: 10.1016/j.jbspin.2009.03.012
58. Ji L, Li T, Chen H, Yang Y, Lu E, Liu J, et al. The crucial regulatory role of type I interferon in inflammatory diseases. *Cell Bioscience*. (2023) 13:230. doi: 10.1186/s13578-023-01188-z
59. McNab F, Mayer-Barber K, Sher A, Wack A, O'Garra A. Type I interferons in infectious disease. *Nat Rev Immunol*. (2015) 15:87–103. doi: 10.1038/nri3787
60. Schreiber G. The role of type I interferons in the pathogenesis and treatment of COVID-19. *Front Immunol*. (2020) 11:595739. doi: 10.3389/fimmu.2020.595739
61. Gerke V, Gavins FNE, Geisow M, Grewal T, Jaiswal JK, Nylandstedt J, et al. Annexins—a family of proteins with distinctive tastes for cell signaling and membrane dynamics. *Nat Commun*. (2024) 15:1574. doi: 10.1038/s41467-024-45954-0
62. Jia Z, Kang B, Dong Y, Fan M, Li W, Zhang W. Annexin A5 derived from cell-free fat extract attenuates osteoarthritis via macrophage regulation. *Int J Biol Sci*. (2024) 20:2994–3007. doi: 10.7150/ijbs.92802
63. You Q, Ke Y, Chen X, Yan W, Li D, Chen L, et al. Loss of endothelial annexin A1 aggravates inflammation-induced vascular aging. *Advanced Sci (Weinheim Baden-Wuerttemberg Germany)*. (2024) 11:e2307040. doi: 10.1002/advs.202307040
64. Vago JP, Nogueira CR, Tavares LP, Soriani FM, Lopes F, Russo RC, et al. Annexin A1 modulates natural and glucocorticoid-induced resolution of inflammation by enhancing neutrophil apoptosis. *J Leukocyte Biol*. (2012) 92:249–58. doi: 10.1189/jlb.0112008
65. Scannell M, Flanagan MB, deStefani A, Wynne KJ, Cagney G, Godson C, et al. Annexin-1 and peptide derivatives are released by apoptotic cells and stimulate phagocytosis of apoptotic neutrophils by macrophages. *J Immunol*. (2007) 178:4595–605. doi: 10.4049/jimmunol.178.7.4595
66. Shao T, Gao Q, Tang W, Ma Y, Gu J, Yu Z. The role of immunocyte infiltration regulatory network based on hdWGCNA and single-cell bioinformatics analysis in intervertebral disc degeneration. *Inflammation*. (2024). doi: 10.1007/s10753-024-02020-7
67. Xiang Q, Zhao Y, Lin J, Jiang S, Li W. The Nrf2 antioxidant defense system in intervertebral disc degeneration: Molecular insights. *Exp Mol Med*. (2022) 54:1067–75. doi: 10.1038/s12276-022-00829-6
68. Xiao L, Xu SJ, Liu C, Wang J, Hu B, Xu HG. Sod2 and catalase improve pathological conditions of intervertebral disc degeneration by modifying human adipose-derived mesenchymal stem cells. *Life Sci*. (2021) 267:118929. doi: 10.1016/j.lfs.2020.118929
69. Honda K, Yanai H, Negishi H, Asagiri M, Sato M, Mizutani T, et al. IRF-7 is the master regulator of type-I interferon-dependent immune responses. *Nature*. (2005) 434:772–7. doi: 10.1038/nature03464
70. Marić I, Durbin JE, Levy DE. Differential viral induction of distinct interferon-alpha genes by positive feedback through interferon regulatory factor-7. *EMBO J*. (1998) 17:6660–9. doi: 10.1093/emboj/17.22.6660
71. Sato M, Hata N, Asagiri M, Nakaya T, Taniguchi T, Tanaka N. Positive feedback regulation of type I IFN genes by the IFN-inducible transcription factor IRF-7. *FEBS Lett*. (1998) 441:106–10. doi: 10.1016/S0014-5793(98)01514-2
72. Koroth J, Buko EO, Abbott R, Johnson CP, Ogle BM, Stone LS, et al. Macrophages and intervertebral disc degeneration. *Int J Mol Sci*. (2023) 24:1367. doi: 10.3390/ijms24021367
73. Chen L, Dai M, Zuo W, Dai Y, Yang Q, Yu S, et al. NF- κ B p65 and SETDB1 expedite lipopolysaccharide-induced intestinal inflammation in mice by inducing IRF7/NLR-dependent macrophage M1 polarization. *Int Immunopharmacol*. (2023) 115:109554. doi: 10.1016/j.intimp.2022.109554
74. He J, Yang Q, Xiao Q, Lei A, Li X, Zhou P, et al. IRF-7 is a critical regulator of type 2 innate lymphoid cells in allergic airway inflammation. *Cell Rep*. (2019) 29:2718–2730.e6. doi: 10.1016/j.celrep.2019.10.077
75. Zhou Q, Lavorgna A, Bowman M, Hiscott J, Harhaj EW. Aryl hydrocarbon receptor interacting protein targets IRF7 to suppress antiviral signaling and the induction of type I interferon. *J Biol Chem*. (2015) 290:14729–39. doi: 10.1074/jbc.M114.633065

Glossary

IDD	Intervertebral disc degeneration	AIP	Aryl Hydrocarbon Receptor Interacting Protein.
LBP	low back pain	UMAP	Uniform Manifold Approximation and Projection
AF	Annulus fibrosus	NLR	Nod-like receptor
NP	Nucleus pulposus		
CEP	Cartilaginous endplate		
NPC	Nucleus pulposus cell		
GEO	Gene Expression Omnibus		
PCA	Principal component analysis		
PC	Principal component		
SNN	Shared Nearest Neighbor		
t-SNE	t-distributed stochastic neighbour embedding		
ssGSEA	Single sample gene set enrichment analysis		
GSEA	Gene set enrichment analysis		
SVM-RFE	Support Vector Machine-Recursive Feature Elimination		
MDA	Mean decrease accuracy		
MDG	Mean decrease Gini		
IREA	Immune Response Enrichment Analysis		
DEG	Differentially expressed genes		
PPI	Protein-protein Interaction		
STRING	Search Tool for the Retrieval of Interacting Genes		
GO	Gene Ontology		
KEGG	Kyoto Encyclopedia of Genes and Genomes		
BP	Biological Process		
MF	Molecular Function		
CC	Cellular Component		
ceRNA	Competing endogenous RNA		
RBP	RNA-binding protein		
TRRUST	Transcription Regulatory Relationships Unraveled Sentence-based Text Mining		
FBS	Fetal bovine serum		
siRNA	Small interfering RNA		
SD	Sprague-Dawley		
MRI	Magnetic resonance imaging		
DHI	Disc height index		
HE	Hematoxylin-eosin		
SO&FG	Safranin O-Fast Green		
BSA	Bovine serum albumin		
Pro_NP	Progenitor nucleus pulposus		
GSVA	Gene Set Variation Analysis		
TF	Transcription factor		
ECM	Extracellular matrix		
CMAP	Connectivity Map		
APC	Antigen-presenting cell		
MMP	Matrix metalloproteinase		
GC	Glucocorticoid		
POLR2A	RNA polymerase II subunit A		
IRF7	Interferon regulatory factor 7;NLR, Nod-like receptor		